

## ABSTRACT

JADELIS, CHRISTOPHER THOMAS. Investigation of Experimental Movement Type and Effort Level Selection for Personalization of a Wrist Musculoskeletal Model. (Under the direction of Dr. Katherine Saul).

This dissertation investigates the effect of different experimental movement conditions and participant relative effort in the creation of personalized wrist musculoskeletal models and evaluates the clinical utility of the predicted computational muscle parameters generated by these personalized models. Computational musculoskeletal models have the potential to augment existing clinical assessments of hand function, enable quantitative tracking of the effectiveness of rehabilitative therapies, and serve as the basis for model-based control of wearable robotics. However, computational models seldom leave the research setting as the parameters used to inform them are derived from cadavers and population averages, limiting their applicability to individual persons. Additionally, direct measurement of muscle parameters on individuals may be costly, invasive, or impractical. Indirect methods of model personalization have been successfully applied to the lower limb; however, due to functional and architectural differences, the information necessary to inform personalization of upper limb models, specifically those of the wrist, has not been comprehensively determined.

We investigated the sensitivity of specific muscle parameters in a wrist musculoskeletal model including optimal fiber length, maximum isometric force, tendon slack length, and fiber pennation angle, to different movement types and participant effort levels able to be measured experimentally. Our results determined specific experimental conditions, suggesting that tendon slack length and optimal fiber length are most influential during isotonic muscle contractions, while maximum isometric force is equally influential under all tested experimental conditions.

Additionally, we found that increasing participant effort level did not significantly increase sensitivity for any of the muscle model parameters examined.

Secondly, we investigated the effect of different movement and effort level training data on the performance of personalized wrist musculoskeletal models to predict joint torques for a range of both high effort and low effort tasks. We examined a group of 10 participants that conducted isometric and isotonic wrist flexion movements to 25% and 50% of their maximum relative effort. Personalized models were generated using simple linear and strength scaling methods as well as a custom joint dynamics informed optimization using both singular movement and effort data, as well as combinations of movement data for singular effort levels. We determined that for the optimized models, models trained using combined sets of both isotonic and isometric contractions for light effort levels provided minor benefits for predictions of joint torques over a range of tasks, but that simple linear scaling is sufficient to capture this functional behavior in healthy populations.

Lastly, we evaluated the clinical relevance of personalized computational musculoskeletal models by determining the linear correlation between model predicted muscle behavior and measured in vivo muscle architecture. We examined personalized models generated from five participants using joint dynamics informed optimization, as well as linear and strength scaling methods. We correlated the model predicted muscle fiber lengths, tendon lengths, and maximum isometric force estimates, with in vivo ultrasound measured muscle belly lengths, external tendon lengths, and muscle cross sectional areas respectively. These correlations revealed that muscle fiber lengths and tendon lengths significantly and positively correlated for all model types, with a modest increase in correlation for the optimized model trained using isotonic movement data and 50% of a participant's relative effort. However, maximum isometric

force was only significantly correlated for the optimized model cases, suggesting that optimization informed models may capture architectural changes not predicted by simple linear or strength scaling. These results suggest that optimization informed personalized models may have clinical applications for quantitatively evaluating muscle specific architectural changes.

© Copyright 2025 by Christopher Thomas Jadelis

All Rights Reserved

Investigation of Experimental Movement Type and Effort Level Selection for Personalization of  
a Wrist Musculoskeletal Model

by  
Christopher Thomas Jadelis

A dissertation submitted to the Graduate Faculty of  
North Carolina State University  
in partial fulfillment of the  
requirements for the degree of  
Doctor of Philosophy

Mechanical Engineering

Raleigh, North Carolina  
2025

APPROVED BY:

---

Dr. Katherine Saul  
Committee Chair

---

Dr. Derek Kamper

---

Dr. Scott Ferguson

---

Dr. Helen Huang

## **DEDICATION**

To my parents, Loretta and Thomas for your love and support as I undertook this degree and through all my pursuits in life, and to my friends, both old and new, that have supported and guided me over all these years.

## **BIOGRAPHY**

Christopher Thomas Jadelis was born in Livingston, New Jersey before moving to Apex, North Carolina where he would later attend Cary Academy. Upon graduating from high school, he would pursue a Bachelor of Science in Biomedical and Health Sciences Engineering at the University of North Carolina at Chapel Hill, which he received in 2017. He began his graduate studies at North Carolina State University in the fall of 2018 in the Department of Mechanical and Aerospace Engineering, completing his Master of Science in Mechanical Engineering in December of 2020 under the direction of Dr. Katherine Saul, and will complete the requirements for his Ph.D. in Mechanical Engineering in December of 2025.

## ACKNOWLEDGMENTS

As I reflect on the past seven years that I have spent as both a master's and a PhD student, I would not have been able to learn, experience, and pursue as much as I have without the guidance, support, and love of so many along the way. The professional insights from faculty and dedicated advisors, as well as the camaraderie and support from friends, colleagues, and family, made this experience possible and I would not be who I am today without them.

First it is with my deepest thanks that I would like to acknowledge my advisor, Dr. Katherine Saul. Your support and guidance through the years that I've spent at NC State, ranging from when I first took your mechanics of human movement class to presenting this dissertation have been invaluable. Your patience, positive and encouraging attitude, and endless support have shaped the way that I pursue research, and I don't think I would have been able to have done half of what I have without your ability to keep both my experiments and writing on track. From responding to all my google chats and making sense of all the odd tangents that I can be prone to go on, your support has made me a better engineer and scientist, and hopefully one that is able to tell a cohesive and concise story.

I also would like to thank my committee members, Dr. Kamper, Dr. Huang, and Dr. Ferguson, for their support and evaluation of this dissertation. I would also specifically like to thank Dr. Kamper for all your support both in this work and in my master's thesis, your technical insight has been essential to my understanding of the biomechanics of the hand and made all the difference in my simulations. I also want to thank Dr. Ferguson for all your insight into adapting the optimization tools I have available to address the challenges presented in this dissertation, and for always challenging me to get at the "why" behind the science and tool development.

I would also like to thank all the members of the MoBL lab, with a special thank you to Dr. Morgan Dalman. Morgan, your curiosity and leadership skills are inspiring, and I am glad to be able to call you a friend. From fun lab meetings over Zoom during Covid, to bouncing ideas around in the office, getting lunch and mid-day breaks, to introducing me to different analysis methods made the studies presented here possible.

I also need to express my deepest thanks to the members of the Aerial Robotics Club. When I first arrived at NC State in 2018, they have been an essential social and technical outlet, allowing me to explore topics and be a part of a team completely unrelated to my other studies. I will always cherish memories of flying at Dorthea Dix on Fridays, flight testing, and late-night cookout runs in the back of David's truck. David, Ethan, Grady, Hannah, Henry, Hailey, Grey, Adam, Phillip, and so many more, I am so glad to have met you and called each of you friends. Much of my research work here would also not have been possible without your insight, and the ability to make use of the undergraduate fabrication lab for tools and equipment. Whenever I needed an oscilloscope, multimeter, or the odd m3 screw, I always knew where to find one, even if those probably should have been used in building Akela or Kavik instead.

I also cannot thank all my friends from undergrad enough that have been with me all this time. Jack, Christina, and all my classmates from the BME class of 2017, thank you for being my friends, the endless hours of studying in Davis library and working on projects in the BME lab are incredibly fond memories, and I don't know if I would have made it through undergrad without your support. Jack, thank you for always checking in on me when I have been having a bad day. I am grateful for all the times that you've given me advice and for all your support through the years. I would also like to thank Phil and the other members of CEMALB at UNC.

My experiences as an undergraduate working in Mucociliary Clearance and Aerosol Research Laboratory shaped and inspired me to pursue research as a graduate student.

Lastly, I want to thank my parents, Tom and Loretta, for being present throughout this process. For listening to me ramble about difficulties in the lab, meals offered, and weekend lunches. Your endless support and patience have made all this possible.

There are still countless other friends and family that have supported me through the years that I haven't named, and I am grateful for all of the experiences that I have had while at NC State. This has been really fun, and I got to contribute to and make some pretty cool things. I'm glad that I was able to pursue research in biomechanics, as well as take time to pursue interests at an advanced level that I would have otherwise never been able to do. It's the kind of thing that makes you glad you stopped and smelled the pine trees along the way you know?

## AUTHORSHIP STATEMENT

The chapters included in this dissertation would not have been possible without the crucial insights and contributions of co-authors. Chapters 2 and 4 both have contributions from co-authors. Chapter 2 “Parameter Sensitivity to Experimental Data Types for Personalizing a Wrist Musculoskeletal Model” includes contributions from Dr. Morgan Dalman: Manuscript review (supporting), conceptualization (supporting), software (supporting). Chapter 4 “In vivo ultrasound assessment of computationally predicted wrist muscle architecture” includes contributions from Dr. Amy Adkins: Conceptualization (supporting), methods development (supporting), data collection (supporting). Additionally, the development of all chapters was supervised by Dr. Katherine Saul: Conceptualization (equal), methods development (supporting), software (supporting), review and editing (equal). Generative artificial intelligence (AI) tools, specifically “Grammarly” and “ChatGPT” were used in the creation of this dissertation. “Grammarly” was used for general grammar and writing assistance including the correction of typos and sentence structure. “ChatGPT” was used to assist in the development of code snippets to perform the repeated measures analysis of variance tests shown in chapters 2 and 3. All outputs from these tools were interpreted and validated by the authors, and all software contributions were validated against the original documentation for the software being used to ensure the correctness of the workflow.

## TABLE OF CONTENTS

LIST OF TABLES .....	ix
LIST OF FIGURES .....	x
<b>Chapter 1: Introduction</b> .....	1
Background .....	1
Modeling Skeletal Muscle with Computational Muscle Models.....	3
Musculoskeletal Model Personalization Techniques.....	9
Specific Aims.....	12
Structure of Dissertation .....	15
<b>Chapter 2: Parameter Sensitivity to Experimental Data Types for Personalizing a Wrist Musculoskeletal Model</b> .....	17
Abstract .....	17
Introduction.....	18
Methods.....	20
Results.....	27
Discussion .....	33
<b>Chapter 3: Investigation of Experimental Task Types for Parameter Estimation in a Wrist Musculoskeletal Model Using a Numeric Optimization Approach</b> .....	36
Abstract .....	36
Introduction.....	38
Methods.....	40
Results.....	47
Discussion .....	51
<b>Chapter 4: Correlation of Computationally Predicted Wrist Muscle Parameters and In-Vivo 3D Ultrasound Measurements</b> .....	54
Abstract .....	54
Introduction.....	55
Methods.....	57
Results.....	62
Discussion .....	66
<b>Chapter 5: Conclusions</b> .....	70
Contributions.....	70
Applications .....	72
Future work.....	73
<b>References</b> .....	75
<b>Appendices</b> .....	83
<b>Appendix A. Additional Statistics for Chapter 2</b> .....	84
<b>Appendix B. Comparison of Movement Type for Chapter 3</b> .....	85

## LIST OF TABLES

Table 2.1	MSK Parameter Sampling Range for Morris Screening .....	26
Table 2.2	MSK Parameter Mean Sensitivity Indices Across Data Types .....	31
Table 2.3	MSK Parameter ANOVA Across Data Types .....	31
Table 2.4	MSK Parameter Sensitivity Pairwise Analysis (Main Effects).....	32
Table 2.5	Parameter Sensitivity ANOVA Across Muscles .....	32
Table 3.1	Optimization and Control Model Case Data Types .....	43
Table 3.2	MSK Optimization Parameter Boundaries (Percent from Nominal Value).....	44
Table 3.3	NRMSE Evaluation ANOVA Results.....	49
Table 3.4	Pearson's Correlation Coefficient Evaluation ANOVA Results.....	49
Table 4.1	Optimization and Control Model Case Data Types (Chapter 3) .....	60
Table 4.2	MSK Model Pearson's Correlation Coefficients .....	63
Table 4.3	MSK Model Mean Difference and Limits of Agreement .....	64

## LIST OF FIGURES

Figure 1.1	Illustration of a muscle fiber and sarcomere complex at resting (optimal) length.....	5
Figure 1.2	Illustration of a “Hill” type muscle model .....	6
Figure 1.3	Illustration of the force length relationship of muscle .....	7
Figure 1.4	Illustration of the force velocity relationship of muscle.....	7
Figure 1.5	Hand wrist MSK model adapted from (McFarland et al., 2022) .....	8
Figure 2.1	Placement of sEMG wet electrodes .....	21
Figure 2.2	Experimental Postures .....	22
Figure 2.3	Mean sensitivity indices overall .....	28
Figure 2.4	Mean absolute sensitivity indices per muscle .....	29
Figure 2.5	Heat map of the pairwise significant relationships between muscle parameters .....	30
Figure 3.1	Flowchart of data preparation.....	42
Figure 3.2	Flowchart of multistep optimization .....	46
Figure 3.3	Average Pearson’s correlation coefficients for all personalized models .....	47
Figure 3.4	Normalized root mean squared error (NRMSE) for all personalized models.....	48
Figure 3.5	Representative evaluation of moment data for optimized and control models .....	50
Figure 4.1	Experimental postures and motion capture marker locations during ultrasound .....	58
Figure 4.2	Representative ultrasound images of muscle anatomical cross-sectional areas.....	59
Figure 4.3	Pearson’s correlation and best fit lines of a representative optimized model and both control model cases .....	65

## CHAPTER 1: Introduction

Hand and wrist function are essential for conducting activities of daily living (ADLs), and can be severely impaired by neurologic and musculoskeletal injuries (Duruöz, 2014; Ghassemi and Kamper, 2022). As a result, developing effective therapies to restore hand function is a common clinical topic in occupational therapy, orthopedics, and stroke rehabilitation (Almkvist Muren et al., 2008; Ghassemi and Kamper, 2022). However, as the hand and wrist support a wide range of complex tasks, quantitative assessment of hand function is challenging, with clinical analysis typically limited to subjectively prescribed and evaluated inventory tests, that can determine general functional ability, but have limited utility in determining the biomechanical basis for specific impairments (Dang et al., 2011; Sacks et al., 2010).

Computational musculoskeletal (MSK) models provide an important tool that promises to augment these clinical assessments. These models enable prediction of individual muscle contributions to functional tasks and provide insight into the benefit of specific rehabilitation strategies. Additionally, these models enable simulation of assistive devices, such as wearable robotics, and their ability to increase functional ability (Akbas and Sulzer, 2019; McCain et al., 2021). However, current MSK models of the hand and wrist are generic, informed by cadaveric data sets or limited in vivo measurements representative of a fiftieth percentile male (Holzbaur et al., 2005; Rajagopal et al., 2016). This limits their clinical utility, as functional capacity may vary substantially across individuals (Holzbaur et al., 2007). Direct measurements of muscle architectural features using medical imaging or intraoperative measures for specific individuals could address this limitation; however, these are often expensive, invasive, or impractical to perform.

Recently, personalization of musculoskeletal models using numeric optimization or machine learning techniques have offered a potential inexpensive and readily available alternative (Berman et al., 2023a; Fregly et al., 2012; Fregly, 2021; Pizzolato et al., 2015). These methods enable indirect prediction of MSK parameters that can more accurately estimate person-specific functional ability in comparison to generic models. These methods have been successfully applied to the lower limb and torso for more accurate prediction of joint torques and kinematics in tasks such as cyclic gait and lifting of objects (Hammond et al., 2025a; Pizzolato et al., 2015). However, the hand and wrist differ considerably from the lower limb in muscle architecture, types of functional tasks performed, as well as the types of measurements that are available to inform model personalization (Goislard De Monsabert et al., 2018; McFarland et al., 2022). As a result, it is unclear if personalization techniques and experimental tasks analogous to those performed in the lower limb are suitable to develop personalized models of the hand and wrist. It is currently unknown which types of experimental tasks reveal the most information about MSK parameters in the hand and wrist, and which combinations of experimental data enable accurate personalization of a hand and wrist model. Lastly, as personalization techniques have currently focused on improving predictions of functional outcomes such as joint torques and kinematics, it is unclear whether MSK parameters estimated using these personalization approaches correlate meaningfully with real world muscle architectural features.

The overall objective of this dissertation is thus to advance MSK model personalization methods of the hand and wrist by (1) determining the relative importance of MSK parameters and experimental task selection in model functional output, (2) investigating the suitability of the identified parameter and experimental task sets for personalization of a wrist MSK model, and

(3) determine if the MSK parameters predicted through indirect MSK model personalization are physiologically meaningful when compared with in vivo ultrasound measurements.

The remainder of this introduction chapter presents pertinent background information on computational muscle models and techniques used for indirect personalization that assist in motivating the latter chapters. This introduction chapter concludes with the focus and specific aims of this dissertation.

## **Modeling Skeletal Muscle with Computational Muscle Models**

### 1.1 Architectural properties of Skeletal Muscle

Computational MSK models simulate realistic movement arising from muscle electromechanical activity, which can provide insight into limb function and identify biomechanical contributors to disability and impairment (Binder-Markey et al., 2019; Holzbaur et al., 2005; McFarland et al., 2022). To perform this, MSK models must implement mathematical representations that capture the force-producing properties of skeletal muscle. Skeletal muscle is composed of bundles of muscle fibers called fascicles, with each muscle fiber containing repeating units of force-generating structures called sarcomeres (Rassier, 2017). Sarcomeres are composed of overlapping filaments of actin and myosin proteins that interact to generate active force, as well as elastic titin proteins that passively resist changes in muscle length (Figure 1.1). During muscle contraction, myosin filaments attach to exposed active sites on actin filaments and engage in a pulling motion that shortens the entire sarcomere unit and the length of the muscle fiber. As this is dependent on the number of active sites available for myosin to interact with, and as actin-myosin interactions are not instantaneous, active force production is dependent on the percentage overlap of the actin and myosin filaments, as well as the contraction velocity of the muscle fiber. This results in the existence of an optimal fiber

length at which the greatest amount of isometric muscle force is able to be produced. This occurs when the maximum number of interaction sites are exposed, overlapping, and the muscle contraction velocity is zero. The maximum amount of force able to be produced in this state is denoted as the maximum isometric force of a muscle.

To exert torque on body joints, and thus produce functional movement, muscle fibers insert into collagenous tissues called tendons that transmit muscle forces across body segments to actuate joints. Muscle fibers insert into these tendons at an angle, referred to as the fiber pennation angle, resulting in the final tendon forces being a function of the muscle forces multiplied by the cosine of the fiber pennation angle. Lastly, these tendons are characterized by non-linear force transmission behavior, where for small tendon excursions, collagen fibers within the tendon must first “uncrimp”, followed by a linear force transmission region once the collagen fibers within the tendon are fully stretched. The length of the tendon immediately before this force transmission occurs is the length at which the tendon is under no strain, referred to as the tendon slack length.

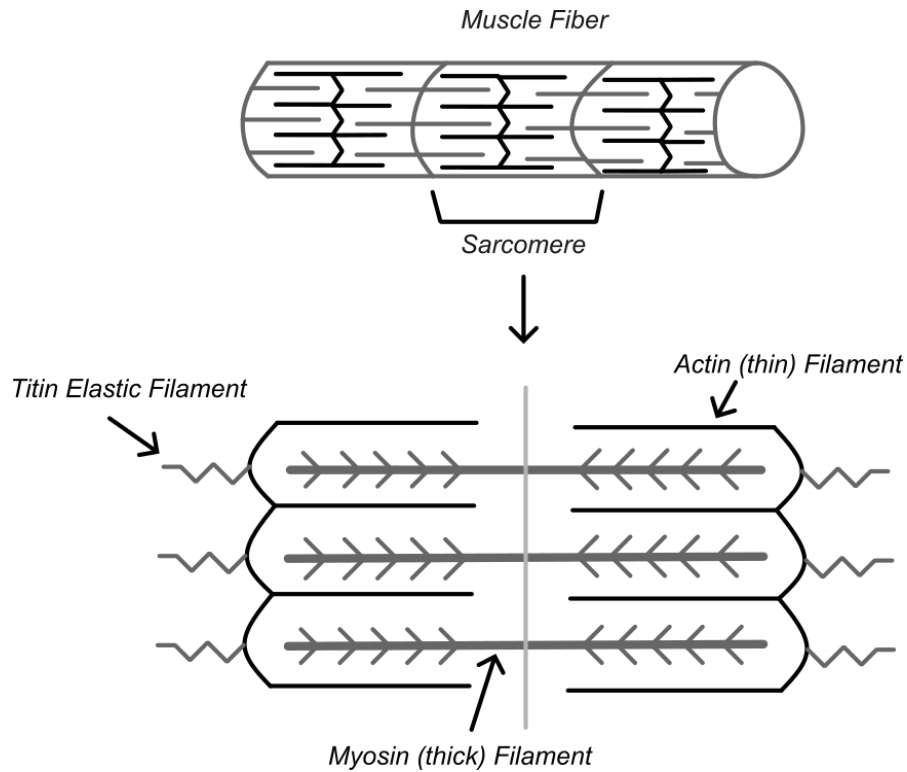


**Figure 1.1** Illustration of a muscle fiber and sarcomere complex at resting (optimal) length.

## 1.2 Computational Muscle Models

To represent the parameters described in the previous section, computational muscle models implement mathematical representations to approximate muscle force production. The earliest muscle model formulation that has been widely adopted and iterated upon is the “Hill” muscle model introduced by physiologist Archibald Vivian Hill (Hill, 1938). This model represents muscle architectural features with a three-element formulation consisting of an active contractile element in parallel with a passive elastic element, which both act upon an elastic spring tendon at an angle representing a uni-pennate muscle (Figure 1.2).

Within this dissertation, the muscle model used in all computational MSK models is the Millard damped equilibrium muscle model (Millard et al., 2013). This model further defines the contractile element to be dependent on muscle fiber length and muscle contraction velocity, as well as a maximum isometric force parameter. Each of these are informed from spline curves

fitted to experimental data. These include a force-length relationship (Figure 1.3) and force-velocity relationship (Figure 1.4). The Millard model also implements passive muscle stiffness, a non-linear elastic tendon, and a muscle fiber damping term to speed convergence in simulation. The simulated tendon is defined by a passive force-length curve and a scalar value representing the tendon slack length. Lastly, the Millard model implements muscle activation dynamics as a first order differential equation to enable control over muscle effort while accounting for the electromechanical delay observed between an initial neural excitation and muscle contraction based on the initial formulations described by (Thelen, 2003; Winters, 1995; Zajac, 1989).

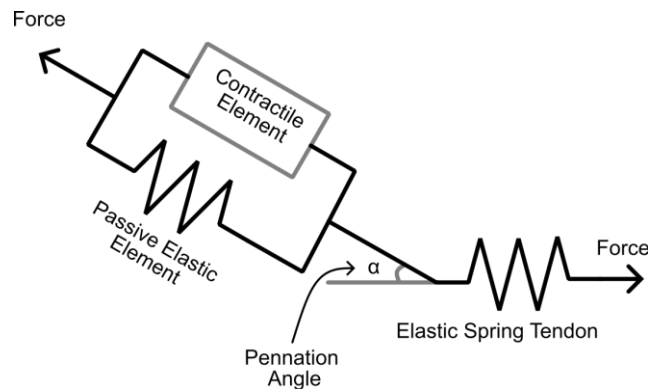


**Figure 1.2** Illustration of a “Hill” type muscle model consisting of a contractile element, parallel passive elastic element, and an elastic spring tendon.

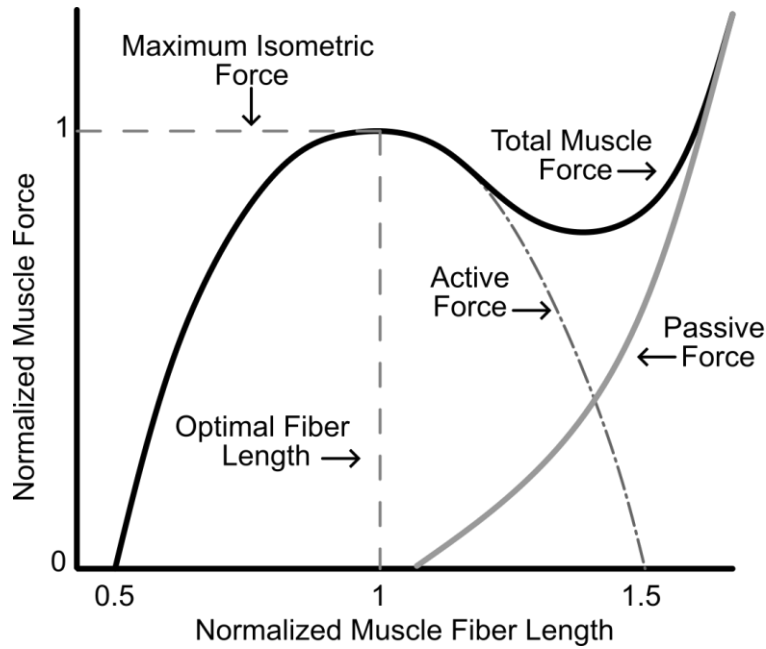


**Figure 1.3** Illustration of the force length relationship of a muscle.

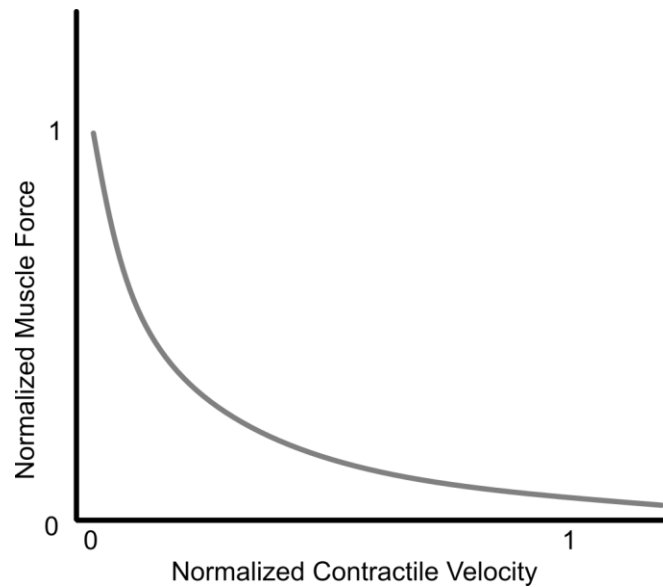


**Figure 1.4** Illustration of the force-velocity relationship of a muscle in the concentric (shortening) domain.

### 1.3 Musculoskeletal Model of the Hand and Wrist

The wrist MSK model used for this dissertation is an adapted version of the wrist hand MSK model developed by (McFarland et al., 2022). This model incorporates muscle definitions for 43 muscles and 23 degrees of freedom governing the forearm and hand; however, for the

purposes of this dissertation, a subset of 5 muscles governing the forearm are examined in detail, including the extensor carpi ulnaris (ECU), extensor carpi radialis longus and brevis (ECRL and ECRB), the flexor carpi ulnaris (FCU), and flexor carpi radialis (FCR) (Figure 1.5). This model was augmented by including additional degrees of freedom representing forearm pronation and elbow flexion to better reflect experimental postures, with joint definitions adapted from the upper limb model presented in (Saul et al., 2015). This model was implemented in the widely adopted biomechanical simulation software OpenSim (Delp et al., 2007), using version 4.4 of the software. This model is composed of rigid bodies representing the bones of the human skeleton, with properties of mass and inertia, linked together by rotational joints. The muscle models are represented as one dimensional muscle paths operating in three dimensions, that follow a geometric path representative of the effective line of action of the muscle being represented. In addition to bony segments and muscle representations, this model additionally includes passive damping forces about each joint representative of soft tissue structures that contribute to joint stability.

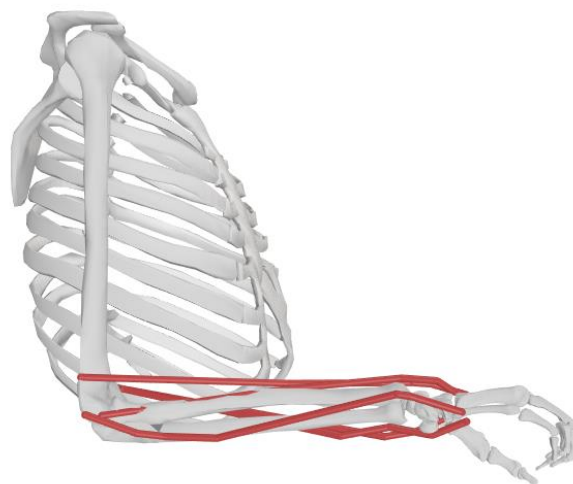


**Figure 1.5** Hand wrist MSK model adapted from (McFarland et al., 2022).

## Musculoskeletal Model Personalization Techniques

### 1.4 Scaling Methods

The MSK model parameters used to inform the model described in the previous section are primarily derived from cadaveric and limited in vivo studies (Holzbaur et al., 2005; McFarland et al., 2022). Because these parameters represent population averages and are not reflective of any specific individual, personalization of these generic models is desirable to better match the anthropometric proportions and to better capture joint movement and loading. However, direct measurement of muscle parameters and bony geometry may be invasive or require expensive medical imaging, making direct personalization impractical. A simple and commonly adopted method of personalization is to simply apply linear scaling factors to each body segment. These scaling factors may be derived from direct measurements of participant anthropometry, such as participant body mass, and external measurements of the long axis of each body segment to be scaled. Geometric scale factors may also be derived through the minimization of the difference between experimental and simulated motion capture markers using the ScaleTool in OpenSim (Delp et al., 2007).

Applying these scaling factors enables simple scaling of body segment mass, inertia, and geometric dimensions, as well as the simple scaling of length-dependent muscle parameters such as optimal fiber length and tendon slack length. These scaling methods however do not enable the scaling of maximum isometric force, as this is not dependent on the long axis lengths of each body segment, and is variable per individual. Simple approaches to address this have previously been performed by measuring an individual's maximum voluntary joint torque during a maximum voluntary contraction (MVC) trial, and applying scale factors to muscles of the same functional group such that the sum of the maximum isometric force of each muscle multiplied by

their respective moment arms is equal to the participant's maximum voluntary joint torque in the experimental posture during the MVC trial (McFarland et al., 2019). However, as each of these methods applies uniform scaling factors, these methods assume that an individual's muscle parameters are proportional to the population average values, which may not be reflected in individuals with altered muscle architecture due to injury or disease. For the purposes of this dissertation, we use both of these simple scaling methods to create control models for comparison to MSK models generated using numeric optimization.

### 1.5 Imaging Methods

Current best practice methods for MSK model personalization that allow for direct measurement or indirect calculation of a limited number of muscle parameters is to make use of medical imaging technologies such as magnetic resonance imaging, micro endoscopy and extended field of view ultrasonography (Adkins et al., 2020; Kainz et al., 2021; Lichtwark et al., 2018). These imaging modalities enable quantification of muscle fascicle length and fiber pennation angle, as well as muscle volume and estimates of muscle physiologic cross-sectional area which can be used to calculate maximum isometric force. True optimal fiber lengths cannot be calculated without information on sarcomere length, which are currently only obtained using micro endoscopy or laser diffraction methods, which are rare and are minimally or surgically invasive. Determination of tendon slack length is also unavailable via traditional imaging methods and requires fitting of muscle-tendon unit lengths to experimental data, as determination of a tendon's resting length is challenging in vivo. While these methods do enable direct measurement of certain muscle parameters, these techniques require imaging expertise and access to expensive equipment, limiting their broad adoption.

## 1.6 Indirect MSK Parameter Prediction Methods

Recently, indirect methods of MSK parameter estimation based on numeric optimization and machine learning techniques such as reinforcement learning have been developed that avoid the limitations of the previous sections. These methods make use of clinically accessible equipment including surface electromyography probes (sEMG), force plates, and dynamometers for experimental data collection, and iteratively compute MSK parameter sets that minimize the difference between simulated and experimentally measured endpoints. These endpoints include joint moments or joint kinematics calculated during forward dynamics simulations with an MSK model as part of these methods respective cost or reward functions (Berman et al., 2023a; Hammond et al., 2025a; Hinson et al., 2022; Pizzolato et al., 2015). These methods are desirable, as they enable indirect estimation of muscle parameters that reflect an individual's functional capacity. As each forward dynamics simulation is being driven by normalized sEMG, wherein each muscle's relative effort is limited by experimental observations, any individual muscle is prevented from being overrepresented in force production. However, while these predictive methods avoid the use of direct medical imaging or invasive measurement techniques, limited work has been performed to validate the predicted MSK parameters generated by these methods.

Additionally, as each muscle may have multiple parameters to optimize, the dimensionality of the optimization problem can be considerably high. As a result it is unlikely to encounter a global solution using local gradient-based optimization approaches, and the evaluation of each objective function call can be computationally expensive. Thus, the use of global optimization approaches such as simulated annealing are necessary to avoid local solutions (Pizzolato et al., 2015). Due to computational constraints, for the purpose of this dissertation, a Bayesian optimization approach based on Bayesian inference methods (van Ravenzwaaij et al., 2018), was

adopted for the generation of optimized MSK models. This was chosen as Bayesian optimization treats each MSK parameter as a Gaussian process model and evaluates a surrogate function to determine each MSK parameter iteration, rather than necessitating the evaluation of the objective function. This reduces the total number of objective function calls while still enabling effective searching of the solution space.

### **Specific Aims**

This dissertation has 3 specific aims to investigate the influence of experimental task selection on personalization of a wrist MSK model, and whether optimization informed MSK models correlate with in vivo muscle architectural features.

**Specific Aim 1: Determine the sensitivity of individual muscle parameters on wrist MSK model response with respect to varying experimental movement conditions and increasing relative effort levels. Motivation:** The diversity of functional tasks performed by the hand and wrist differs considerably from tasks performed by the lower limb, with hand and wrist tasks characterized by non-cyclic highly dynamic tasks that encompass a range of effort levels from free kinematic motion to high effort grasping and lifting. Thus, it is unknown which types of experimental tasks are suitable to inform muscle parameters in a wrist MSK model for use in parameter optimization. Additionally, as muscle architectural features in the forearm differ from those in the lower limb, with characteristics of small pennation angles, long tendons, and small cross-sectional areas, it is unclear which MSK parameters are of specific importance in parameter optimization, and which parameters may be fixed at their mean physiologic values.

**Methods:** We conducted a sensitivity analysis using a Morris Screening approach (Morris, 1991) to evaluate the sensitivity of wrist flexion prediction accuracy to changes in muscle parameters under different movement and effort conditions using data collected from 10 participants. These

data included sEMG, wrist flexion angles, and wrist flexion moment information from participants performing muscle contractions under isometric and isotonic movement conditions at 25% and 50% of the maximum relative effort. **Hypothesis 1:** Optimal fiber length and tendon slack length will be more sensitive under isotonic conditions at all effort levels. **Hypothesis 2:** Maximum isometric force and fiber pennation angle will be most sensitive under increased effort conditions for both movement types.

**Specific Aim 2: Evaluate the performance of personalized wrist MSK models informed using optimization-based methods when trained using varying combinations of experimental movement type and effort level data. Motivation:** Current optimization-based approaches for personalization of wrist MSK models rely solely on sEMG and kinematics data to inform their objective functions (Han et al., 2025; Hinson et al., 2022); however, as the range of dynamic tasks performed with the hand and wrist may encompass movements that require considerable effort, it is unknown if kinematics-driven approaches, without the inclusion of experimentally measured joint dynamics, are able to inform muscle parameters that enable robust prediction of both high and low effort tasks under differing movement conditions. Additionally, as muscle parameters may be influenced differently by varying experimental movement and effort conditions, it is unclear how these experimental data or combinations of experimental data may influence the performance of optimization-informed MSK models in predicting a range of task types conducted at increasing effort levels. **Methods:** We evaluated the joint torque prediction accuracy of personalized wrist MSK models for 10 participants, trained on combinations of isometric and isotonic movements under 25% and 50% of each participant's maximum voluntary effort. Each personalized MSK model was evaluated against individual isometric or isotonic data sets at both 25% and 50% relative effort to determine the accuracy of

each estimated parameter set at predicting both light and moderate effort tasks for varying movement conditions. These models were additionally compared against control models that were personalized using conventional linear scaling techniques to determine the benefit of optimization-informed approaches over simpler methods. **Hypothesis:** Isotonic muscle contractions performed with light resistance will yield a parameter set that most accurately predicts joint moments under all movement and effort conditions.

**Specific Aim 3: Investigate the correlation between MSK parameters predicted with both optimization informed methods and conventional scaling with ultrasound imaging measurements to determine physiological relevance. Motivation:** Optimization-based MSK parameter prediction methods typically focus on endpoint prediction accuracy, such as the prediction of joint moments or kinematics, without validating the estimated muscle parameters. Additionally, the computational muscle models used in these MSK models must make simplifying assumptions about muscle architecture, such as assuming unipennate muscles with uniform muscle fiber lengths, resulting in computational predictions not being directly reflective of underlying physiology. Thus, whether the computational parameters predicted by these personalization approaches significantly correlates with in vivo muscle architecture is unknown. **Method:** We collected and evaluated ultrasound images collected at specific muscle landmarks, sEMG, and dynamometry data from 5 participants. We generated personalized MSK models informed using an optimization method that minimized the differences between experimental and simulated wrist flexion moment under isometric and isotonic movement conditions for 25% and 50% of each participant's maximum voluntary effort, as well as personalized models using conventional linear scaling methods. We correlated the reported muscle fiber lengths, tendon lengths, and estimated maximum isometric force parameters for each personalized model, with

approximate measurements of muscle belly length, external tendon length, and muscle cross sectional areas derived from the ultrasound images.

**Hypothesis:** Significant and positive correlations between personalization predicted and experimental measurements will be larger for optimization-informed approaches in comparison to linear scaling, with the highest correlations observed for optimized models trained using isotonic movement data regardless of effort level.

### **Structure of Dissertation**

This dissertation consists of three chapters, with chapters 2-4 presenting the above aims. These chapters take the form of independent journal articles in preparation for publication. Chapter 2: “Parameter Sensitivity to Experimental Data Types for Personalizing a Wrist Musculoskeletal Model” Christopher Jadelis, MS; Morgan Dalman, PhD; Katherine R. Saul, PhD (In preparation for the Journal of Biomechanics, 2026) presents an investigation into the sensitivity of muscle parameters in a wrist MSK model to varying movement and effort conditions. Chapter 3 “Investigation of Experimental Movement Types and Effort Levels on the Performance of Personalized Wrist Musculoskeletal Models” Christopher Jadelis, MS; Katherine R. Saul, PhD (In preparation for the Journal of Biomechanics, 2026) presents an investigation into the effect of varying movement and effort conditions on the joint moment prediction accuracy of optimization informed wrist MSK models. Chapter 4: “In vivo ultrasound assessment of computationally predicted wrist muscle architecture” Christopher Jadelis, MS; Amy Adkins, PhD; Katherine R. Saul, PhD (In preparation for the Journal of Biomechanics, 2026) presents an investigation into the correlation of muscle parameters predicted using personalization methods with in vivo muscle architectural features. In Chapter 5, I conclude the

dissertation with a summary of significant findings, potential impact and suggest future avenues of research.

## CHAPTER 2

### **Parameter Sensitivity to Experimental Data Types for Personalizing a Wrist**

#### **Musculoskeletal Model** (In preparation for the Journal of Biomechanics, 2026)

Christopher Jadelis, MS; Morgan Dalman, PhD; Katherine R. Saul, PhD

#### **Abstract**

Computational musculoskeletal (MSK) models are valuable tools for simulating functional movement and resulting deficits from injury or deformity. However, these models seldom leave the research setting due to difficulty in personalizing MSK models to individuals especially for joints of the upper limb such as the wrist. Because of the diversity of upper limb tasks, it remains unclear which types of experiments are most informative for estimating MSK parameters, thereby preventing standardization in experimental task selection. To address this, we conducted a sensitivity study using Morris Screening with experimental data collected from 10 participants performing static and dynamic muscle contractions under 25% and 50% of their voluntary effort.

We examined an MSK model of wrist flexion that included the extensor carpi radialis longus and brevis (ECRL and ECRB), extensor carpi ulnaris (ECU), and the flexor carpi radialis and ulnaris (FCR and FCU) muscles. Parameters for each muscle included their maximum isometric force, optimal fiber length, tendon slack length, fiber pennation angle, and fiber damping. We found that isotonic contractions were most effective for inducing a sensitive parameter response for all parameters. Participant effort, however, had a minimal and statistically insignificant effect on parameter sensitivity. Maximum isometric force, tendon slack length, and optimal fiber length substantially influenced model response and are thus important

to include in personalization schemes, while pennation angle and fiber damping for these muscles were non-influential within their physiological range. These results provide insight into experimental data collection and standardization of methods for use in personalization of MSK models of the wrist and upper limb.

## **Introduction**

Computational musculoskeletal (MSK) models have been effective research tools for studying how changes in neuromuscular control, musculoskeletal architecture, bone morphology, and muscle geometry affect function in clinical populations due to injuries or deformities (Binder-Markey et al., 2019; Dalman et al., 2022; Holzbaur et al., 2005; Kainz et al., 2021). However, MSK models are seldom deployed directly in clinical settings as diagnostic tools (Smith et al., 2021). One persistent obstacle to implementing MSK models directly in clinical settings is the difficulty in tailoring MSK models to specific individuals (Žuk et al., 2018). Current average or generic MSK models typically derive muscle paths, geometry, and MSK parameters from cadaveric dissection or limited in vivo studies reliant on expensive or scarce medical imaging techniques (Saul et al., 2015; Scheys et al., 2008b). Additionally, certain MSK parameters, such as tendon slack length, cannot be directly measured.

Recent work in MSK model personalization has focused on the use of numeric optimization techniques to predict MSK parameters from indirect, non-invasive, and less expensive measurements of limb function during task performance that are more feasible to implement in a clinical setting (Ao et al., 2023; Fregly et al., 2012; Hammond et al., 2025b; Pizzolato et al., 2015). While these approaches have successfully demonstrated the reproduction of experimental joint torques for models of the lower limb, such as the knee (Bennett et al., 2022), challenges remain for adapting these techniques more generally to other parts of the body.

For example, personalization of lower limb models typically relies on ground reaction forces (GRFs) measured during cyclic gait or dynamic running experiments to inform joint dynamics as part of parameter optimization (Bennett et al., 2022; Pizzolato et al., 2015; Tagliapietra et al., 2015). The upper limb, by contrast, and specifically the wrist, experiences non-cyclic, highly dynamic movement without the means to easily measure forces analogous to GRFs. Thus, in lieu of GRFs, current studies personalizing the wrist and hand use a variety of measurements, including free-hand motion without joint torque measurement, or limited dynamometry studies for measuring torque about singular joints (Barry et al., 2022; Conrad and Kamper, 2012; Crouch and Huang, 2016; Dwivedi et al., 2020). As these approaches vary substantially both in the types of measurements taken and parameters estimated, it is unclear what types of experiments provide the most or best information to inform parameter estimation, and which parameters are important. Previous studies using sensitivity analyses have examined the robustness of the MSK parameter prediction to uncertainty in measurement, and for refinement of MSK parameter prediction (Hinson et al., 2022; Žuk et al., 2018), but none have examined how parameter sensitivity responds to different classes of movement and loading conditions. Because of the diversity of upper limb tasks, it remains unclear which types of experiments are most informative for estimating MSK parameters, preventing standardization in experimental task selection.

The objective of this work is to investigate the effectiveness of different movement and loading conditions to induce sensitive MSK-muscle-tendon parameter response in a wrist MSK model, using wrist dynamometry to apply static and dynamic task conditions under different levels of exertion. In addition, we sought to ascertain which MSK parameters were most influential for model response and thus critical for inclusion in designs of personalization schemes. We hypothesized that dynamic conditions would be necessary to induce a sensitive

response for MSK parameters dependent on muscle length and contraction speed (such as tendon slack length, muscle optimal fiber length, and muscle fiber damping). Additionally, we hypothesized that higher exertions would induce the most sensitive responses for MSK parameters related to peak force-generating capacity (such as muscle maximum isometric force and muscle pennation angle). .

## **Methods**

### **Experimental Data Collection**

Ten able-bodied participants were recruited for this study (5 male and 5 female). Each participant was informed of the study procedures and signed a consent form following a protocol approved by the North Carolina State University Institutional Review Board (IRB protocol number 5493). Anthropometric information - including total body mass, participant height, and anthropometric measurements of the hand, forearm, and upper arm - was collected from each participant. Surface electromyography (sEMG) probes (Noraxon Telemetry DTS, Noraxon, Scottsdale, Arizona) were fitted to each participant over the thickest portion of the wrist flexor and extensor muscles, including the extensor carpi radialis brevis (ECRB), extensor carpi radialis longus (ECRL), extensor carpi ulnaris (ECU), flexor carpi radialis (FCR), and flexor carpi ulnaris (FCU) muscles (Figure 2.1). These muscles were identified via manual palpation while instructing participants to flex and extend their wrist while pressing against a surface to express the muscle belly.

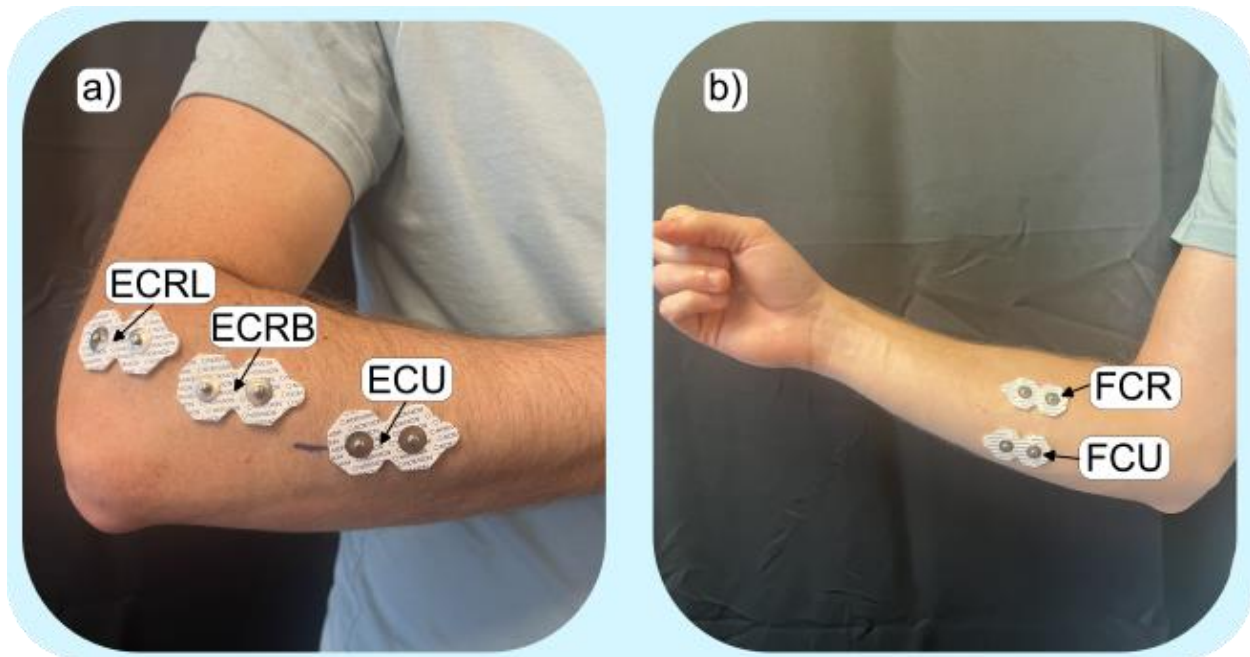


**Figure 2.1** Placement of sEMG wet electrodes for the wrist extensors (a) and wrist flexors (b). This figure purposely omits the sEMG sensors to better show the electrode pad placement.

sEMG was collected from each participant with a sampling frequency of 1500 Hz. The sEMG data were filtered and rectified using a bandpass filter with a passband of 30 to 250 Hz and a moving root mean squared filter with a window of 100 ms. The filtered and rectified signal was smoothed using a 3rd-order Savitzky-Golay filter. sEMG signals were normalized to each participant's relative maximum effort calculated during maximum voluntary contraction (MVC) trials at a wrist flexion posture of zero degrees.

Wrist flexion angle, velocity, and moment production were recorded using a Biodex 4 dynamometer (Biodex Medical Systems, Shirley, New York). Participants were instructed to perform isometric muscle contractions for wrist flexion and extension in three static postures (flexion = 30°, 0°, and -30°, flexion is positive) and dynamic isotonic muscle contractions over a range of motion (wrist flexion = -35° to 35°) (Figure 2.2, row 1). A custom attachment was affixed to the handle of the Biodex dynamometer to allow participants to flex and extend their wrist without using their fingers to grasp the handle, limiting interference from the finger flexors

and extensors. Muscle contractions were performed to 25% and 50% of each participant's maximum moment-generating capacity. Relative effort was shown through a live feedback display for isometric trials based on MVC wrist moment. Isotonic trials were conducted with a minimum threshold torque of 25% or 50% of the participant's maximum recorded joint moment. Three repetitions of flexion and extension for each contraction type and effort level were recorded. Each muscle contraction trial was conducted for five seconds, with ten-second rest periods to limit muscle fatigue.

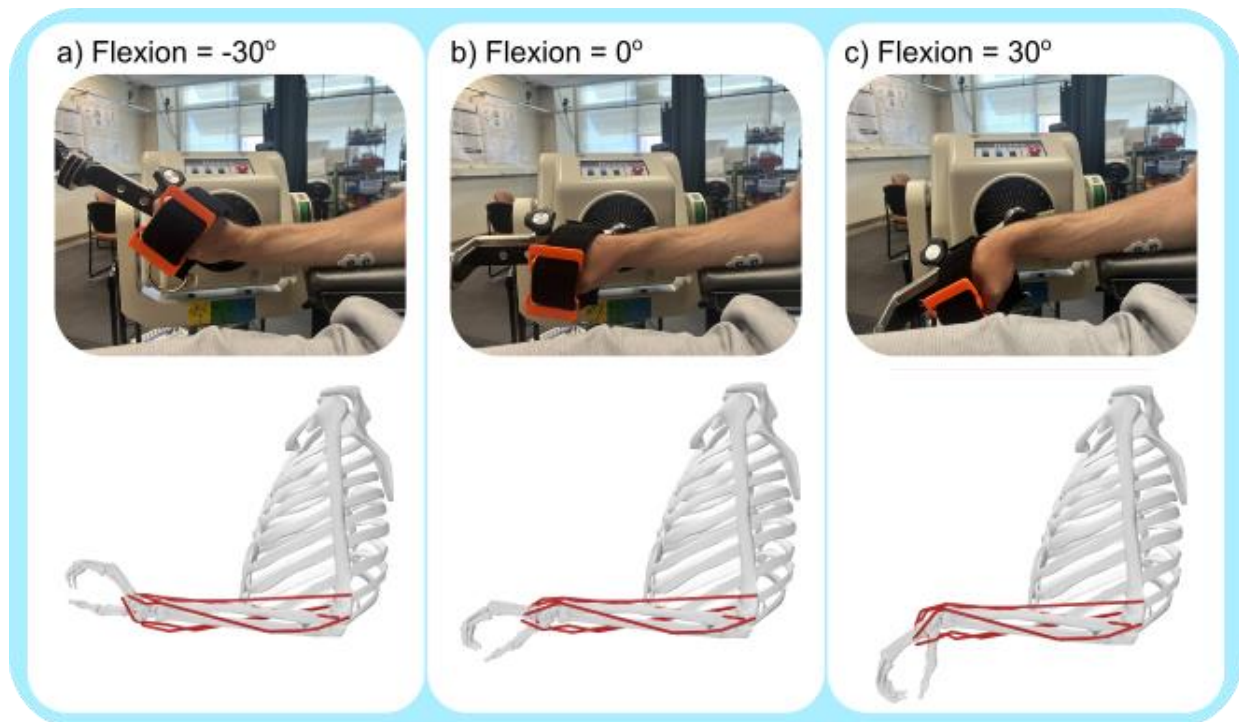


**Figure 2.2** Experimental postures in the Biodex 4 Dynamometer (row 1), and their corresponding model representations (row 2) using a modified hand-wrist model (McFarland et al., 2022).

### **MSK Model Selection and Model Response**

A previously developed MSK model of the wrist and hand was selected for this study to evaluate MSK parameter sensitivity (McFarland et al., 2022). This model was configured and evaluated using OpenSim (version 4.4) (Delp et al., 2007). Each model was configured to have

representations of the wrist flexors and extensors (ECRL, ECRB, ECU, FCR, and FCU), while all other muscle representations were disabled. Joint definitions were configured such that elbow flexion was fixed at 90°, wrist pronation was fixed at 90°, while wrist flexion was prescribed to follow experimental wrist flexion/extension joint angles for each trial. The joints of the fingers were fixed to approximate a grasping posture of the Biodex 4 dynamometer wrist attachment handle (Figure 2.2, row 2).

Scaled versions of the base model were created for each participant using the included OpenSim Scale Tool and participant-specific anthropometry to modify muscle lengths, rigid body segment lengths, and rigid segment masses. Each scaled MSK model was evaluated by performing a series of forward dynamic simulations for each participant, using the included Forward Dynamics Tool in OpenSim, and generated with each experimental movement type and effort level as inputs. Each simulation used the processed sEMG data as muscle excitation, integrating these muscle excitations forward in time to develop muscle forces and joint moments during the prescribed motion. For each forward dynamics simulation, the model response was determined from the difference between simulated joint moments and experimental joint moments according to (equation 2.4).

$$NRMSE = \frac{1}{M} \sum_{m=1}^M \sqrt{\left( \frac{\tau_{exp}(m) - \tau_{sim}(m)}{\max(\tau_{exp})} \right)^2} \quad (2.1)$$

$$Max\ Error = \frac{\max(|\tau_{exp} - \tau_{sim}|)}{\max(|\tau_{exp}|)} \quad (2.2)$$

$$XCorr = \left( 1 - \left( \frac{1}{\sum_{t=1}^T (\tau_{exp}(t))^2} \sum_{t=1}^T \tau_{exp}(t) \tau_{sim}(t) \right) \right) \quad (2.3)$$

$$Model\ Response = NRMSE + Max\ Error + XCorr \quad (2.4)$$

This response function returns a normalized score representing the evenly weighted sum of three components over all trials for each experimental condition, including the normalized root mean squared error (NRMSE; equation 2.1), the normalized maximum error (equation 2.2), and the normalized cross-correlation for the zero-lag case of the simulated and experimental joint moments (equation 2.3).

### Sensitivity Study Description

MSK parameter sensitivity to movement and loading conditions was determined using the Morris Screening method (Morris, 1991). This method was implemented using the SAFE Toolbox (Pianosi et al., 2015) within MATLAB version 2023b (The Mathworks, Natick, Massachusetts). This method was selected as a computationally efficient global sensitivity analysis able to determine the relative importance of model parameters in computationally expensive models. This method is characterized as a “one at a time” (OAT) approach that varies parameters independently over the parameter range to elicit first-order parameter effects. First-order effects for each parameter ( $EE_k$ ) are defined in (equation 2.5), where  $Y(x_i)$  represents the model response defined by the response function (equation 2.4),  $x_i$  represents a vector of MSK parameters, and  $\Delta e_i$  represents a finite step in the direction of a single parameter within its upper and lower bounds. In this study, parameter sample locations were selected using Latin hypercube sampling (LHS), with the number of total simulations ( $K$ ) determined according to (equation 2.6).

$$EE_k = \frac{Y(x_{i...K} + \Delta e_{i...K}) - Y(x_{i...K})}{\Delta_{i...K}} \quad (2.5)$$

$$K = r(m + 1) \quad (2.6)$$

The variable  $m$  corresponds to the number of parameters included in the model (5 parameters per muscle x 5 muscles represented in the model,  $m = 25$ ), and the variable  $r$  corresponds to an

arbitrary scaling factor. In this study, the value of  $r$  is chosen to be 25 ( $r = 25$ ) to effectively sample each parameter over its physiologically plausible range (Table 2.1), resulting in a total of  $K = 650$  simulations per experimental movement type (2 types) and effort level (2 levels).

Each of the 650 simulations used different parameter values selected from a feasible physiologic range, with bounds determined based on prior literature (Table 2.1). Bounds are expressed as a percentage of the nominal value; this is required because optimal fiber length and tendon slack length had different nominal values for each participant due to the initial anthropometric scaling process. Bounds for optimal fiber length, tendon slack length, and pennation angle were set at three standard deviations from the nominal values as reported by (Lieber et al., 1992, 1990). Bounds for maximum isometric force parameters were determined to be proportional to three standard deviations above the mean wrist flexion moment reported in (Holzbaur et al., 2007) (upper bound) the lowest wrist flexion moment reported in (Holzbaur et al., 2007) (lower bound); the lower bound was chosen to avoid the case of zero maximum isometric force being assigned to any given muscle. Bounds for fiber damping, as described in (Millard et al., 2013), were defined to correspond with a lower bound of 0 (no damping) and upper bound of 0.1 (OpenSim default value), with a nominal value of 0.06 as determined from preliminary forward dynamics simulations. The bounds for pennation angle and fiber damping listed in parentheses in Table 2.1 indicate narrower bounds used for a singular participant to ensure simulation convergence and avoid an invalid zero fiber length case.

Table 2.1: MSK Parameter Sampling Range for Morris Screening (Percent from Nominal Value)

Parameter					
Bounds	Optimal Fiber Length (%)	Tendon Slack Length (%)	Maximum Isometric Force (%)	Pennation Angle (%)	Fiber Damping (%)
Lower Bound	82.20%	86.80%	42%	0% (25%)	0%
Upper Bound	117.80%	113.20%	251.40%	216%	200% (150%)

Each elementary effect index calculated via the Morris Method is used to calculate three global sensitivity measures:  $\mu_i$ ,  $\mu_i^*$ , and  $\sigma_i$ , representing the mean sensitivity index, the absolute mean sensitivity index, and the standard deviation of the sensitivity indices for each parameter, respectively (equations 2.7, 2.8, and 2.9). Values of  $\mu_i$ ,  $\mu_i^*$  indicate a parameter's independent effect on model response, while  $\sigma_i$  correlates to the level of interaction of that parameter with other parameters. Values for  $\mu_i^*$  and  $\sigma_i$  are reported, while values for  $\mu_i$  are used for the calculation of  $\sigma_i$  (equation 2.9).

$$\mu_i = \frac{1}{k} \sum_{j=1}^k EE_i^j(x) \quad (2.7)$$

$$\mu_i^* = \frac{1}{k} \sum_{j=1}^k |EE_i^j(x)| \quad (2.8)$$

$$\sigma_i = \frac{1}{k-1} \sum_{j=1}^k (EE_i^j(x) - \mu_i)^2 \quad (2.9)$$

Sensitivity indices are unitless but approximately correspond to the average change in model response with respect to a given parameter. A larger sensitivity index ( $\mu_i^*$ ) indicates a greater change in model response per incremental change in a given parameter, while a larger standard deviation ( $\sigma_i$ ) indicates greater interaction between parameters. A larger sensitivity index is desirable, as it indicates that the parameter elicits a stronger model response, providing more information about how incremental parameter changes influence model response (equation 2.4).

## Data Analysis

Sensitivity indices were calculated for each MSK parameter for each muscle and participant for each of the contraction types (2 types) and effort levels (2 types). To evaluate whether task type affected parameter sensitivity, the sensitivity indices were each averaged across all muscles and participants and evaluated using a two-way repeated measures analysis of variance (ANOVA) with main effects of contraction type and effort level, and their interactions, using a within-subjects model to account for variability across trials for the same participant. In addition, muscle-specific sensitivity indices were compared using a similar ANOVA to determine if differences existed in parameter sensitivity among muscles. Pairwise comparisons of sensitivity indices were conducted between each movement type and effort level pair for both average and muscle-specific sensitivity indices using a post-hoc multiple comparisons test with a Bonferroni correction, to determine specific group differences. Parameters with a non-zero but very small ( $\mu_i^* < 0.05$ ) sensitivity index were considered non-influential to the model response, while parameters with a larger sensitivity index were considered influential.

## Results

### Mean Sensitivity Indices

Mean sensitivity indices ( $\mu^*$ ) for maximum isometric force, optimal fiber length, and tendon slack length (Table 2.2) all had measurable effects on model response ( $\mu^* > 0.1$ ) and are thus considered influential parameters. Tendon slack length and maximum isometric force affected normalized torque response by greater than 53% and 18% respectively ( $\mu^* > 0.53$  and 0.18) under dynamic motion for both effort cases. Optimal fiber length, while less influential, was still sensitive and affected the model response by greater than 14% ( $\mu^* > 0.14$ ) according to (equation 2.4) in our simulations. Fiber pennation angle and fiber damping were minimally

influential on model response ( $\mu^* < 0.1$ ) and are thus non-influential parameters. The repeated measures ANOVA showed significant differences between movement type for all sensitive parameters ( $p < 0.05$ ), with higher sensitivity indices observed for isotonic contractions (Figure 2.3). No significant differences were observed between effort levels. However, significant interactions between movement type and effort level ( $p < 0.05$ ) were observed for optimal fiber length (Table 2.3). Post-hoc pairwise comparisons demonstrated that movement type influenced the magnitude of the sensitivity indices for optimal fiber length and tendon slack length, with isotonic contractions having the highest sensitivity ( $p < 0.05$ ). However, contraction type did not have an effect on the sensitivity of maximum isometric force ( $p > 0.05$ ; Table 2.4). Effort level affected the influence of tendon-slack length sensitivity within the isotonic contraction cases, with a modest increase in average sensitivity for the 25% effort case within the isotonic contractions of 3.4% (difference in  $\mu^* = 0.034$ ). Together, these suggest that isotonic contractions elicit greatest parameter sensitivity among the data types tested, while effort level has minimal effect on parameters aside from tendon slack length.

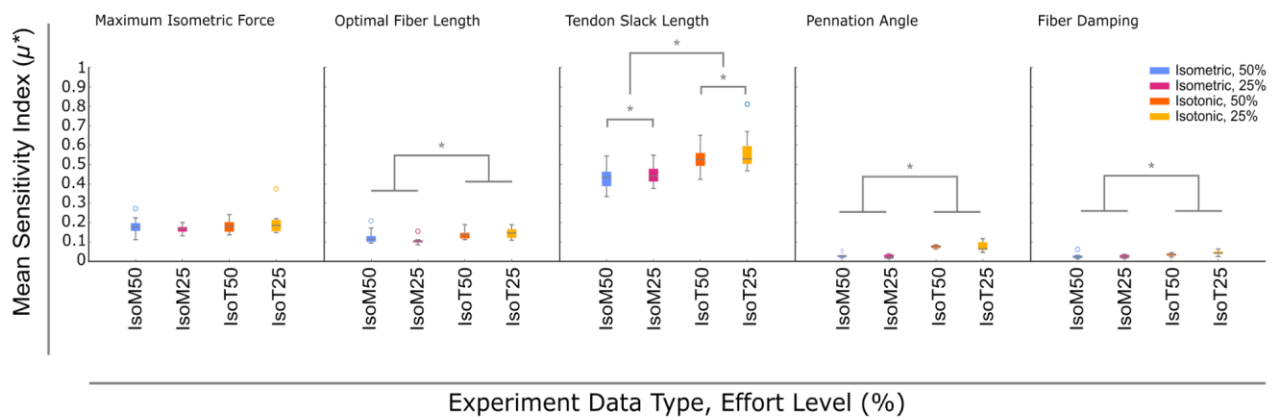


**Figure 2.3** Mean sensitivity indices ( $\mu^*$ ) for the isometric and isotonic 50% and 25% effort cases. Statistically significant differences ( $p < 0.05$ ) between groups are reported as horizontal bars joining respective groups labelled with an asterisk.

## Parameter Sensitivity Per Muscle

As isotonic contractions elicited the greatest parameter sensitivity, further analyses presented here consider the isotonic cases only for comparisons between individual muscles (Figure 2.4). The repeated measures ANOVA revealed significant differences in sensitivity of parameters between muscles ( $p < 0.05$ ; Table 2.5). Pairwise comparisons within the isotonic cases indicated that tendon slack length had significantly greater sensitivity (Figure 2.5) in the FCR, FCU, and ECRB ( $\mu^* > 0.58$ ; Figure 2.4), affecting model response by greater than 58% for these muscles, compared to the ECRL and ECU, which affected model response by greater than 34% ( $\mu^* > 0.34$ ). Maximum isometric force was most influential for the FCU muscle, which influenced model response by greater than 21% ( $\mu^* > 0.21$ ).

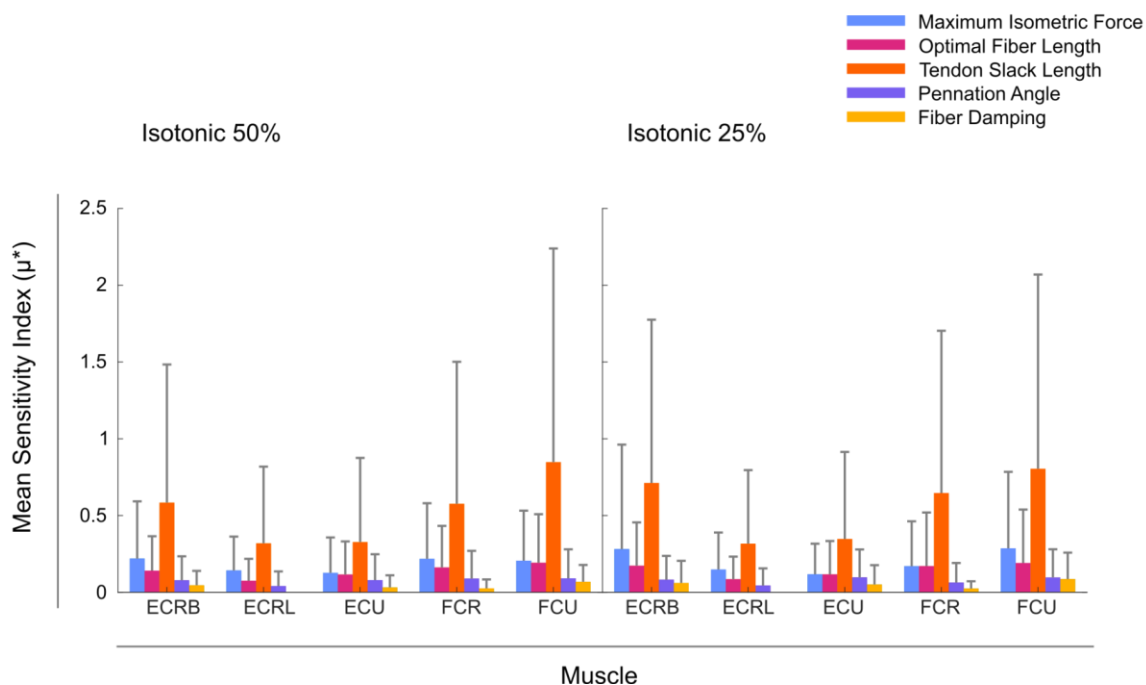


**Figure 2.4** Mean absolute sensitivity indices and standard deviation per muscle for the isotonic contraction cases. Significant relationships between parameters are shown in a separate plot.

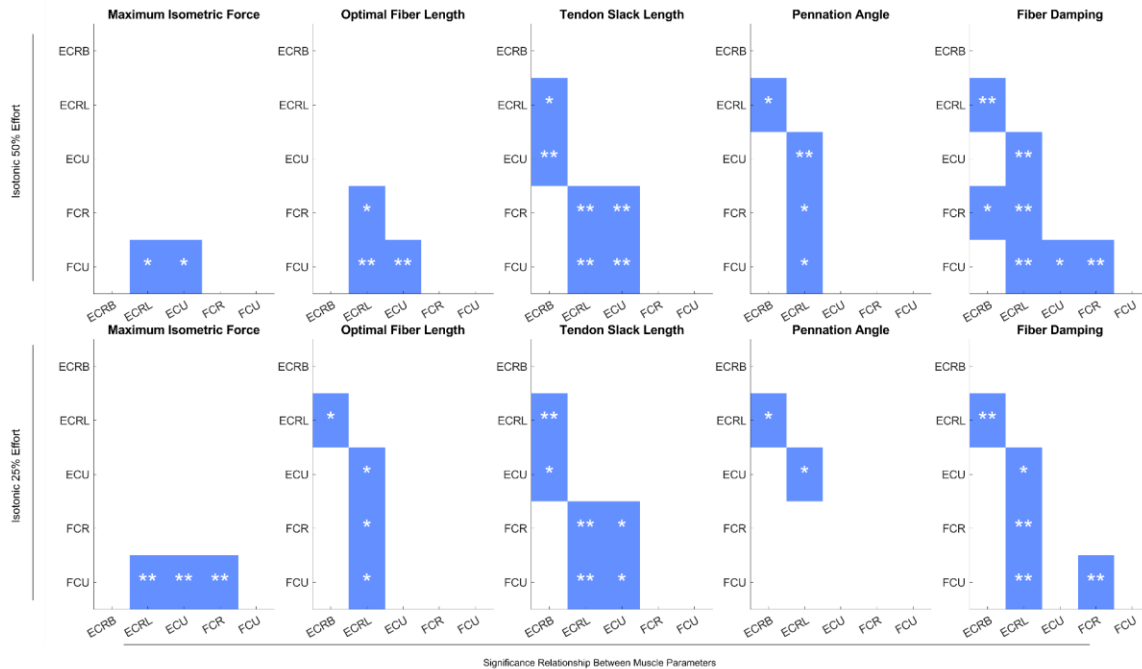


**Figure 2.5** Heat map of the pairwise significant relationships between muscle parameters within the isotonic 50% and isotonic 25% effort cases. A single asterix (\*) indicates a pairwise significant difference with a p-value < 0.05, while two asterisks (\*\*) indicate a difference with a p-value < 0.01.

Table 2.2: MSK Parameter Mean Sensitivity Indices Across Data Types

Parameter	<b>Data Type (Contraction Type, Effort Level)</b>			
	Isometric, 50% Effort ( $\mu^* \pm \sigma$ )	Isometric, 25% Effort ( $\mu^* \pm \sigma$ )	Isotonic, 50% Effort ( $\mu^* \pm \sigma$ )	Isotonic, 25% Effort ( $\mu^* \pm \sigma$ )
Optimal Fiber Length	0.126 ± (0.262)	0.106 ± (0.201)	0.137 ± (0.234)	0.147 ± (0.269)
Tendon Slack Length	0.429 ± (0.670)	0.451 ± (0.752)	0.531 ± (0.853)	0.565 ± (0.887)
Maximum Isometric Force	0.183 ± (0.319)	0.168 ± (0.318)	0.182 ± (0.302)	0.201 ± (0.382)
Pennation Angle	0.029 ± (0.065)	0.025 ± (0.058)	0.075 ± (0.158)	0.076 ± (0.152)
Muscle Fiber Damping	0.026 ± (0.060)	0.026 ± (0.061)	0.034 ± (0.068)	0.044 ± (0.098)

Table 2.3: MSK Parameter ANOVA Across Data Types

Parameter	<b>Factor</b>		
	Contraction Type (F-statistic, p-value)	Effort Level (F-statistic, p-value)	Contraction Type x Effort Level (F-statistic, p-value)
Optimal Fiber Length	<b>5.403, (0.045*)</b>	0.743, (0.411)	<b>6.620, (0.030*)</b>
Tendon Slack Length	<b>21.284, (0.001*)</b>	2.278, (0.166)	0.069, (0.667)
Maximum Isometric Force	1.030, (0.337)	0.022, (0.886)	1.560, (0.243)
Fiber Pennation Angle	<b>107.176, (&lt;0.001**)</b>	0.198, (0.667)	0.258, (0.624)
Fiber Damping	<b>7.122, (0.026*)</b>	2.128, (0.179)	<b>9.534, (0.013*)</b>

Table 2.4: MSK Parameter Sensitivity Pairwise Analysis (Main Effects)

Parameter	Comparison Group	
	Contraction Type (Mean Diff $\pm$ SE, p-value)	Effort Level (Mean Diff $\pm$ SE, p-value)
Optimal Fiber Length	<b>0.026 <math>\pm</math> (0.011), (0.045*)</b>	0.005 $\pm$ (0.006), (0.411)
Tendon Slack Length	<b>0.108 <math>\pm</math> (0.023), (&lt;0.01**)</b>	<b>0.028 <math>\pm</math> (0.019), (0.017*)</b>
Maximum Isometric Force	0.016 $\pm$ (0.016), (0.337)	0.002 $\pm$ (0.011), (0.886)
Pennation Angle	<b>0.049 <math>\pm</math> (0.005), (&lt;0.01**)</b>	0.002 $\pm$ (0.004), (0.667)
Muscle Fiber Damping	<b>0.013 <math>\pm</math> (0.005), (0.026*)</b>	0.005 $\pm$ (0.003), (0.179)

Table 2.5 MSK Parameter Sensitivity ANOVA Across Muscles

Parameter	Contraction Type	
	Isotonic 50% (F-statistic, p-value)	Isotonic 25% (F-statistic, p-value)
Optimal Fiber Length	9.301, (<0.01**)	7.054, (<0.01**)
Tendon Slack Length	16.721, (<0.01**)	18.629, (<0.01**)
Maximum Isometric Force	5.319, (<0.01**)	5.838, (<0.01**)
Fiber Pennation Angle	5.367, (<0.01**)	4.177, (<0.01**)
Fiber Damping	28.202, (<0.01**)	14.025, (<0.01**)

## Discussion

This work identifies types of movement tasks that may be most appropriate for personalizing wrist MSK models, which is important for standardizing data collection approaches for the upper limb. Among the different experimental movement types examined, isotonic contractions elicited the highest parameter sensitivity for optimal fiber length and tendon slack length, and optimal muscle force sensitivity was not affected by task type. Meanwhile, effort level generally had little effect on parameter sensitivity, contrary to our initial hypothesis. Because only tendon slack length sensitivity differed between effort levels and the absolute effect of effort level was marginal, increasing effort level may not improve parameter selection during model personalization according to our analysis.

Within the parameters examined, tendon slack length, optimal fiber length, and maximum isometric force were found to be influential on model response, in line with previous studies (Hinson et al., 2022). Tendon slack length had the largest effect, with an average sensitivity index more than twice that of any other parameter, followed by maximum isometric force and optimal fiber length, respectively. In contrast, fiber pennation angle and fiber damping were not influential ( $\mu^* < 0.1$ ) on model response. This is expected for pennation angle, as its physiological range for the wrist flexor and extensor muscles is narrow, with the maximum previously reported values for wrist muscles being less than  $12.1^\circ$  (Lieber et al., 1990). Muscle fiber damping, while initially expected to play a larger role, was not influential within the prescribed bounds of the no-damping case and the initial default value of 0.1 (Millard et al., 2013). These results suggest that these parameters can be fixed at their mean physiologic or recommended values, as numeric optimization is unlikely to meaningfully alter these parameter values.

Muscle-dependent sensitivity may in part be dependent on differences in their muscle architecture. For example, greater sensitivity in maximum isometric force was detected for FCR, FCU, and ECRB, which have larger cross-sectional areas than the ECRL and ECU (Loren and Lieber, 1995). However, these same muscles had greater sensitivity for tendon slack length compared to ECRL AND ECU, but there is no clear pattern relating this to reported tendon slack length; for example, the ECRB has a shorter tendon than the ECRL, but the ECU has the shortest tendon yet was not very sensitive (Loren and Lieber, 1995). Thus, further investigation is needed to understand how individual muscle architecture affects parameter sensitivity.

Previous work examining parameter sensitivity for different MSK models of the wrist under free-hand motion conditions (Han et al., 2025; Hinson et al., 2022) similarly reported that tendon slack length and maximum isometric force had the greatest influence on model output, with optimal fiber length as less influential. This study extends previous sensitivity analyses by quantifying parameter sensitivity under different experimental data types and effort levels, rather than for a single type of condition. Together, these indicate that tendon slack length, maximum isometric force, and optimal fiber length are necessary to tune for model personalization. These parameters are most informed by isotonic contractions, regardless of effort level, based on individual task performance.

While this study identifies specific experimental conditions that are likely to be effective for use in MSK model personalization, it is not comprehensive of all experimental conditions that may be used to personalize an MSK model of the hand and wrist. This study examines only a single degree of freedom and a subset of muscles in the forearm that govern wrist motion. Previous studies have demonstrated that forearm muscles governing finger motion that span the wrist make significant contributions to wrist flexion and extension (Han et al., 2025), and thus

may play a substantial role. As only isometric and isotonic contractions were examined for wrist flexion, future work may examine the inclusion of additional degrees of freedom at the wrist or multi-joint motion. Additionally, the inclusion of a freehand motion case would enable a more direct comparison to previous studies. Extending the current study would provide additional insight into how more complex movement and additional muscles influence parameter sensitivity.

Overall, this study identifies key muscle parameters important for MSK model personalization and the experimental conditions relevant to the wrist for which these parameters are sensitive. These findings provide a foundation for standardizing experimental data types used in wrist and other upper-limb MSK model personalization and may provide relevant information for future development of optimization tools tailored specifically for MSK models of the hand and wrist.

## CHAPTER 3

### **Investigation of Experimental Movement Types and Effort Levels on the Performance of Personalized Wrist Musculoskeletal Models** (In preparation for the Journal of Biomechanics, 2026)

Christopher Jadelis, MS; Katherine R. Saul, PhD

#### **Abstract**

Personalization of computational musculoskeletal (MSK) models is an important development in computational biomechanics, promising to expand their use as research tools with potential clinical applications. While MSK personalization methods have been developed that successfully predict functional outcomes in the lower limbs, limited work has been applied to personalization of MSK models of the upper limb. One challenge is that lower limb models are usually informed by joint dynamics, while upper limb models are typically limited to kinematics data. Because of this, it is unclear what types of upper limb tasks are sufficient or necessary for robust personalized upper limb model development or functional prediction.

To address this, we developed a joint dynamics-informed optimization tool compatible with previous MSK models in OpenSim and applied it to a wrist MSK model. We obtained wrist flexion data collected from 10 participants conducting isometric and isotonic muscle contractions to 25% and 50% of the maximum voluntary effort. Personalized models were created using these data as training data in isolation and in combination; model performance was assessed by comparing predicted and measured joint moments over the duration of each trial, and performance of models personalized with the optimization tool were compared to performance of models personalized using standard strength or length scaling approaches. Personalized models trained on combined isometric and isotonic data produced the lowest normalized root mean

squared error (NRMSE), improving over simple strength scaled controls but with no significant difference compared to linearly scaled models. Minimal differences were observed among other model experimental movement types and effort levels. These findings suggest that linear scaling may be sufficient to predict general task performance in healthy individuals with strength profiles close to the nominal model. Additional work is needed to evaluate whether personalization via optimization provides additional predictive value in clinical populations where underlying parameters are unlikely to scale linearly with limb anthropometry, or for a wider variety of upper limb tasks.

## Introduction

Electromyography (EMG)-informed personalization of musculoskeletal (MSK) models, performed using numeric optimization and machine learning approaches, has become an important tool in computational biomechanics (Berman et al., 2023a; Hammond et al., 2025c; Kainz et al., 2021; Pizzolato et al., 2015; Sartori et al., 2017, 2018). These methods are of particular interest, as unlike generic MSK models, personalized models enable the prediction of individual-specific functional ability. Personalized predictive models may, therefore, have much greater potential for clinical application, including personalized treatment and rehabilitation plans (Fregly et al., 2012; Stanev et al., 2021), and may provide the foundation for model-based control of wearable robotics for amputees and stroke survivors (Berman et al., 2023a; Ghassemi and Kamper, 2021a; Han et al., 2025). These applications would allow for MSK models to be useful both as scientific research tools and in clinical settings (Fregly, 2021).

However, while recent personalization methods to develop these models have advanced towards clinical applicability, approaches have largely focused on MSK models of the lower extremities, often with emphasis on specific joints such as the knee, with limited work examining other limbs (Bennett et al., 2022; Hammond et al., 2025c; Kainz et al., 2021; Pizzolato et al., 2015; Rook et al., 2025). Some previous work has explored personalizing MSK models for joints in the upper limb, primarily in the wrist (Han et al., 2025; Sartori et al., 2018), using custom workflows. This limitation is due in part to current lower-limb personalization methods being informed by lower-limb specific measurements, such as ground reaction forces (GRFs) used to inform joint dynamics. Analogous reaction forces in the upper limb are often challenging to acquire, as they may necessitate the use of expensive or highly custom equipment (Faber et al.,

2013; Riddle et al., 2020), require highly prescribed upper limb tasks with bespoke measurement systems, or are irrelevant to open chain activities such as reaching and manipulation.

In place of reaction forces and joint dynamics, current efforts for wrist and hand are designed to make use of joint kinematics only. These approaches rely on motion capture or goniometry to track joint kinematics during minimal-effort, kinematic-only motion, and use bespoke workflows with kinematics-driven objective or reward functions to personalize MSK models of the wrist and metacarpophalangeal joints (Berman et al., 2023a; Hinson et al., 2022; Zhao et al., 2023). As these personalization methods utilize kinematics-only motion where muscle forces are minimal, it is unknown if models optimized without the inclusion of joint dynamics are able to predict function for tasks that require higher relative muscle forces and joint moments.

Prior sensitivity studies (Chapter 2) examined different experimental data types and relative effort levels to determine MSK model parameter sensitivity to tasks requiring higher relative muscle forces and joint moments using a joint dynamics informed response function. This study revealed specific parameters - including tendon slack length, maximum isometric force, and optimal fiber length - that are influential to model response under specific movement conditions. However, while sensitivity indices are useful for identifying relative importance of parameters and the presence of non-influential parameters, it remains unknown how varying movement and effort types influence the performance of personalized models in reproducing experimental joint moments in relative high effort tasks.

Thus, to address this we investigate the accuracy and robustness of EMG and joint-dynamics informed personalization using different movement and loading conditions as training data and testing performance with all task types. We hypothesize, based on prior work examining

parameter sensitivity to movement types and effort levels (Chapter 2), that dynamic motion with light resistance, represented here as isotonic contractions performed at 25% of a participant's maximum effort, will most accurately reproduce joint moments under both those and other task conditions.

## **Methods**

### **Experimental Data Collection**

Experimental data used in this study were collected using the protocol described in (Chapter 2); a summary is provided here. Ten able-bodied participants (5 male, 5 female,  $n = 10$ ) were recruited for this study following a protocol approved by the North Carolina State University Institutional Review Board (IRB). Anthropometric data - including height, weight, and the linear dimensions of each segment of the right arm and hand - were collected for each participant. Wrist flexion moment, joint velocity, and flexion joint angle were recorded using a Biodex 4 Dynamometer (Biodex Medical Systems, Shirley, New York) during isometric muscle contractions in three postures (flexion =  $-30^\circ$ ,  $0^\circ$  and  $30^\circ$ ) and isotonic muscle contractions over a range of motion (flexion =  $-35^\circ$  to  $35^\circ$ ). Each movement type was collected at both 25% and 50% of a participant's maximum voluntary effort. Maximum voluntary efforts for flexion and extension were determined during isometric maximum voluntary contractions (MVC) with a wrist flexion posture of  $0^\circ$ . Three repetitions of wrist flexion and extension were performed for each contraction type, effort level, and posture. Normalized surface electromyography was recorded for each participant from the wrist flexor and extensor muscles (ECRB, ECRL, ECU, FCR, and FCU) during all trials. Experiment order was consistent between all participants, with participants performing repetitions of isometric contractions at 25% and 50% of their maximum

effort consecutively, followed by isotonic contractions at 25% and 50% of their maximum effort consecutively, with ten second rest periods between each repetition.

### **MSK Model and Input Data Configuration**

A previously developed MSK model of the hand and wrist developed in OpenSim (Delp et al., 2007) was selected for use in this study (McFarland et al., 2022). This model was implemented and configured in OpenSim version 4.4. The default model was augmented with joint definitions for elbow flexion and wrist pronation derived from a previous OpenSim upper limb model (Holzbaur et al., 2005). Prior to model optimization, a linearly scaled model matching participant anthropometry was generated for each participant using their anthropometric information and the included OpenSim Scale Tool. To replicate the experimental posture of each participant, elbow flexion and wrist pronation were each fixed at 90° (Figure 3.1), and the joints of the fingers were fixed in a grasping posture. Muscle representations of the wrist flexors and extensors (ECRB, ECRL, ECU, FCR, and FCU) were included in each model, while all other muscle representations were disabled. To more accurately represent experimental conditions, a coordinate limit force with a damping parameter of 0.005 Nm/degree/second was included in each model, representing the damping force contributed by the Biodex motor. This damping parameter was determined empirically from constant velocity experiments without participants present to determine the approximate damping coefficient of the Biodex motor.

For each participant, trial-specific data structures for each contraction type and effort level were constructed for use in model optimization; these were composed of the participant's sEMG, flexion moment data, and wrist flexion joint angles (Figure 3.1). Each structure also included trial-specific versions of each participant's model that prescribed wrist flexion angles to

follow the recorded wrist. Each data structure included input data and trial-specific models for two repetitions each of flexion and extension.

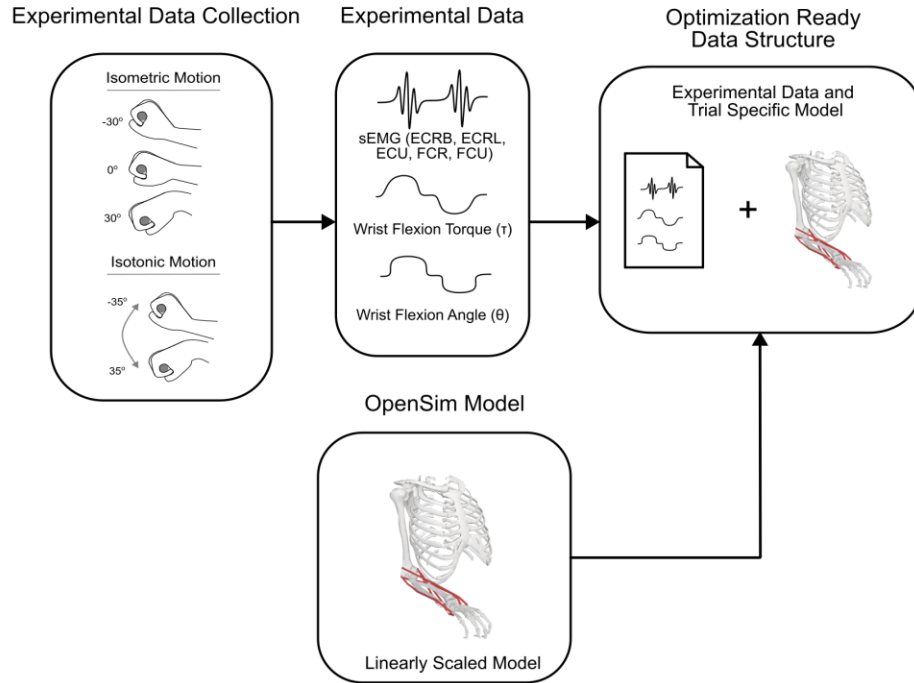


**Figure 3.1** Flowchart of the data preparation process for constructing the input dataset used in the optimization tool. Experimental data is collected, processed, and used to generate a trial-specific version of each participant’s linearly scaled OpenSim model.

### Model Optimization Cases

To evaluate the influence of different experimental data types and participant effort levels on the performance of personalized wrist MSK models, eight different personalized model cases were developed (Table 3.1). These included personalized models trained using isometric or isotonic contractions, and combinations of both contraction types for two effort levels. We also included a cross-trained case in which length dependent parameters (tendon slack length and optimal fiber length) were trained using isotonic contractions, while maximum isometric force was trained using isometric contractions for both effort levels. In addition to the optimized model cases, two control group cases were included. The first control model was an unoptimized,

linearly scaled MSK model, where only tendon slack length and optimal fiber length were linearly scaled using the OpenSim ScaleTool. The second control model was a simple strength scaling based on prior upper-limb scaling methods (McFarland et al., 2019). This strength-scaled model used the ScaleTool for length scaling, and scaled maximum isometric force of each of the flexors and extensors using a shared scaling factor such that the resulting flexion and extension moments generated by each muscle group matched the maximum voluntary contraction moment for flexion and extension.

Table 3.1: Optimization and Control Model Case Data Types

<i>Data Type Used to Inform Muscle Parameters</i>		
<i>Optimized Model Case</i>	<i>Tendon Slack Length, Optimal Fiber Length (Contraction Type, Effort Level)</i>	<i>Maximum Isometric Force (Contraction Type, Effort Level)</i>
Isometric 50%	Isometric, 50%	Isometric, 50%
Isometric 25%	Isometric, 25%	Isometric, 25%
Isotonic 50%	Isotonic, 50%	Isotonic, 50%
Isotonic 25%	Isotonic 25%	Isotonic, 25%
Cross 50%	Isotonic, 50%	Isometric, 50%
Cross 25%	Isotonic, 25%	Isometric, 25%
Combined 50%	Isometric and Isotonic, 50%	Isometric and Isotonic, 50%
Combined 25%	Isometric and Isotonic, 25%	Isometric and Isotonic, 25%
<i>Control Model Cases</i>		
Linearly Scaled Control	Participant Anthropometry (scale factors)	N/A
Strength Scaled Control	Participant Anthropometry (scale factors)	Participant MVC Moment

## **Model Personalization**

Parameters selected for optimization were muscle maximum isometric force, optimal fiber length, and tendon-slack length, based on the results of the sensitivity analysis conducted in Chapter 2. Personalization was conducted in two stages, with each stage using the workflow

described in (Figure 3.2). First, length-dependent parameters (optimal fiber length and tendon-slack length) were optimized to minimize time delay between simulated and experimental joint moments. Second, maximum isometric force was optimized to minimize amplitude differences in joint torque error. Parameter bounds (Table 3.2) were defined according to the same boundaries described in Chapter 2, and expressed as percentage multiples of each parameter’s nominal value. The bounds for optimal fiber length and tendon-slack length were set to three standard deviations from the nominal values reported by (Lieber et al., 1990; Loren and Lieber, 1995). The bounds for maximum isometric force were determined to be proportional to three standard deviations above the mean wrist flexion moment reported by (Holzbaur et al., 2007) and the lowest wrist flexion moment reported in (Holzbaur et al., 2007) (lower bound).

Table 3.2: MSK Optimization Parameter Boundaries (Percent from Nominal Value)

<i>Parameter</i>			
<i>Bounds</i>	Optimal Fiber Length (%)	Tendon Slack Length (%)	Maximum Isometric Force (%)
Lower Bound	82.20%	86.80%	42%
Upper Bound	117.80%	113.20%	251.40%

Note: These bounds in this table are reproduced from (Chapter 2).

### **MSK Model Optimization Workflow**

To generate personalized models of each participant, an optimization workflow (Figure 3.2) was developed and implemented in MATLAB version 2023b (The Mathworks, Natick, Massachusetts). Each personalization was performed by first importing a configured data structure described previously, followed by performing a series of forward dynamics simulations with each trial-specific model using the OpenSim application programming interface (API). Model parameters were optimized for each set of forward dynamics simulations to minimize an objective function (equation 3.4) adapted from the model response function shown in (Chapter

2). The objective function is the sum of three equally weighted components, 1) the normalized root mean squared error (NRMSE; equation 3.1) and 2) maximum error (equation 3.2) between simulated and experimental joint moments to account for moment error over time and maximum error magnitude, and 3) the normalized cross correlation of the simulated and experimental moments for zero lag (equation 3.3) to account for any timewise offset between experimental and simulated joint moments. These components were chosen to capture and minimize errors in overall joint moment magnitude and signal mismatch.

$$NRMSE = \frac{1}{M} \sum_{m=1}^M \sqrt{\left( \frac{\tau_{exp}(m) - \tau_{sim}(m)}{\max(|\tau_{exp}|)} \right)^2} \quad (3.1)$$

$$Max\ Error = \frac{\max(|\tau_{exp} - \tau_{sim}|)}{\max(|\tau_{exp}|)} \quad (3.2)$$

$$XCorr = \left( 1 - \left( \frac{1}{\sum_{t=1}^T (\tau_{exp}(t))^2} \sum_{t=1}^T \tau_{exp}(t) \tau_{sim}(t) \right) \right) \quad (3.3)$$

$$J = NRMSE + Max\ Error + XCorr \quad (3.4)$$

Objective function minimization was conducted in two phases. First, parameters were adjusted using a Bayesian Optimization algorithm, using an expected improvement per second plus acquisition function, configured to run 150 iterations to explore the parameter space and approximate a global minimum. This number of iterations was chosen based on preliminary evaluations showing that the objective does not improve following this number of iterations. Second, the approximate global solution found using Bayesian Optimization was fine-tuned using sequential quadratic programming (SQP) using MATLAB's *fmincon* function. This hybrid approach was chosen, as Bayesian Optimization efficiently identifies likely candidate regions for a global minimum with few function calls, but it does not guarantee convergence to a minimum,

while the SQP approach allows for convergence to the nearest minimum through a gradient-based method to refine the approximate solution given by the Bayesian step.

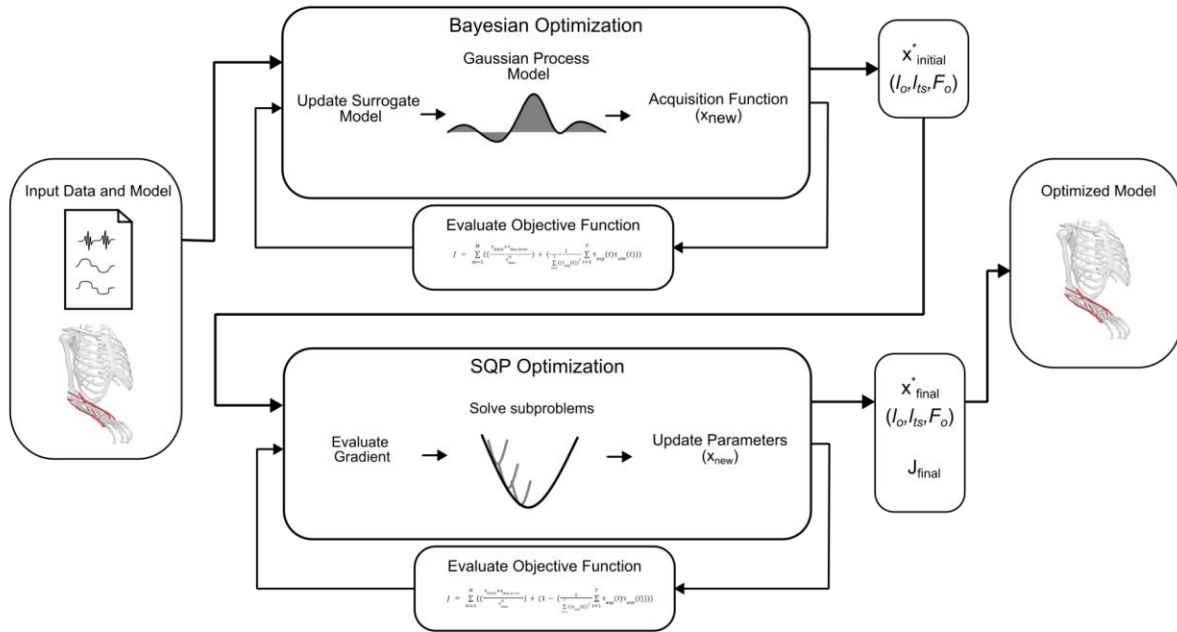


**Figure 3.2** Flowchart of the multi-step optimization process. The input data structure (Figure 3.1) is used as the input for both optimization steps. Bayesian optimization occurs first, and determines an approximate parameter set near the global minimum for use in SQP optimization which is used to refine the parameter set and generate a personalized model.

### Personalized Model Evaluation

To evaluate the performance of each personalized model in comparison to the control models, four sets of forward dynamic simulations were performed for each model. These simulations corresponded to isometric and isotonic contractions for both light and moderate effort. For each evaluation case, the normalized root mean squared error (NRMSE) (equation 3.1) and Pearson's correlation coefficient were reported for each model case for each evaluation type. To assess whether model performance differed based on the training data type and effort level used for optimization, a repeated measures analysis of variance test (ANOVA) was performed using a within-subjects model, with comparisons performed for training data type, effort level, and evaluation case. Pairwise comparisons were performed using a multiple

comparisons post-hoc test using a Bonferroni correction to identify specific differences between models.

## Results

### Personalized Model Evaluation Pearson's Correlation Coefficients

Across all model types for the isometric evaluation, Pearson correlation coefficients were consistently greater than 0.7 for both optimized models and controls. The isotonic contraction evaluations had substantially lower correlation coefficients. Overall, the best performing case was the isotonic 25% effort case, with an average correlation coefficient of 0.77 across all evaluation types (Figure 3.3).

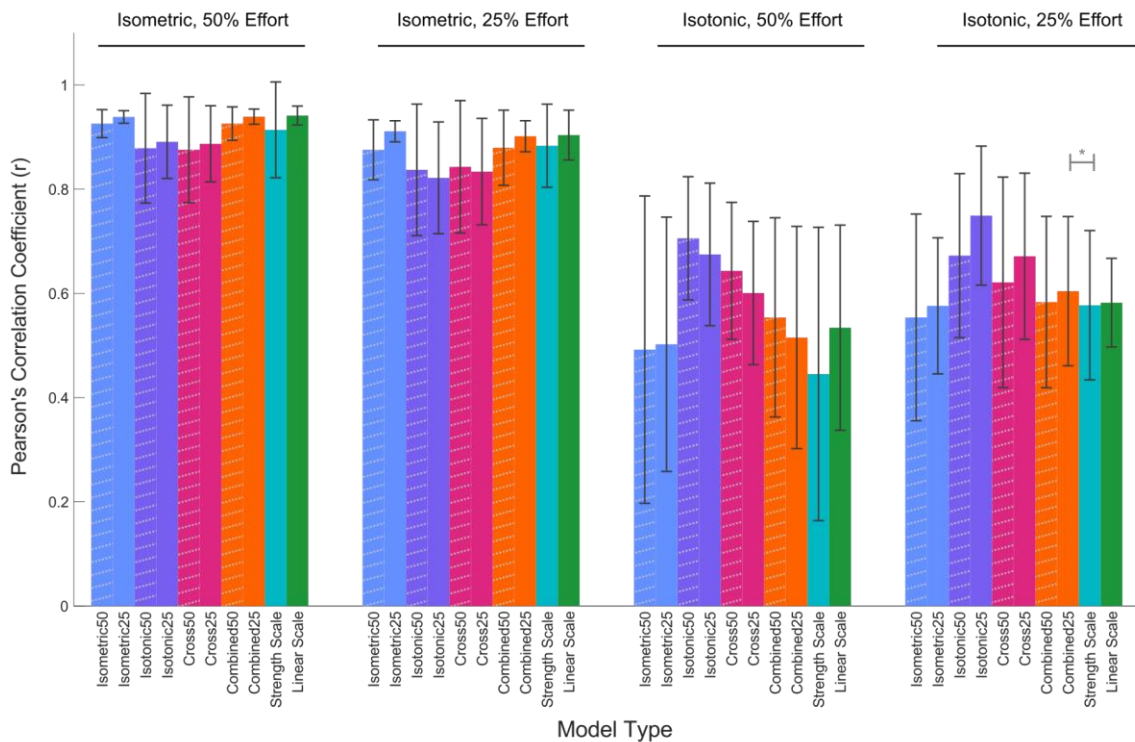


**Figure 3.3** Average Pearson's correlation coefficients for each optimized and control model case, shown for evaluation type. These bars and error bars represent the mean and standard deviation of the correlation coefficients over all study participants.

The repeated measures ANOVA for Pearson's correlation coefficients showed significant differences among model types, evaluation cases, effort levels, and interactions between these ( $p < 0.05$ ; Table 3.3). Pairwise differences were detected between the combined 25% effort model and the strength-scaled control model ( $p = 0.04$ ).

### Personalized Model Evaluation NRMSE

Of the optimized models examined, the case with the lowest average NRMSE was the combined 25% effort case, with average improvements of 9.5% and 17.1% over the linearly scaled and strength-scaled control models, respectively (Figure 3.4).

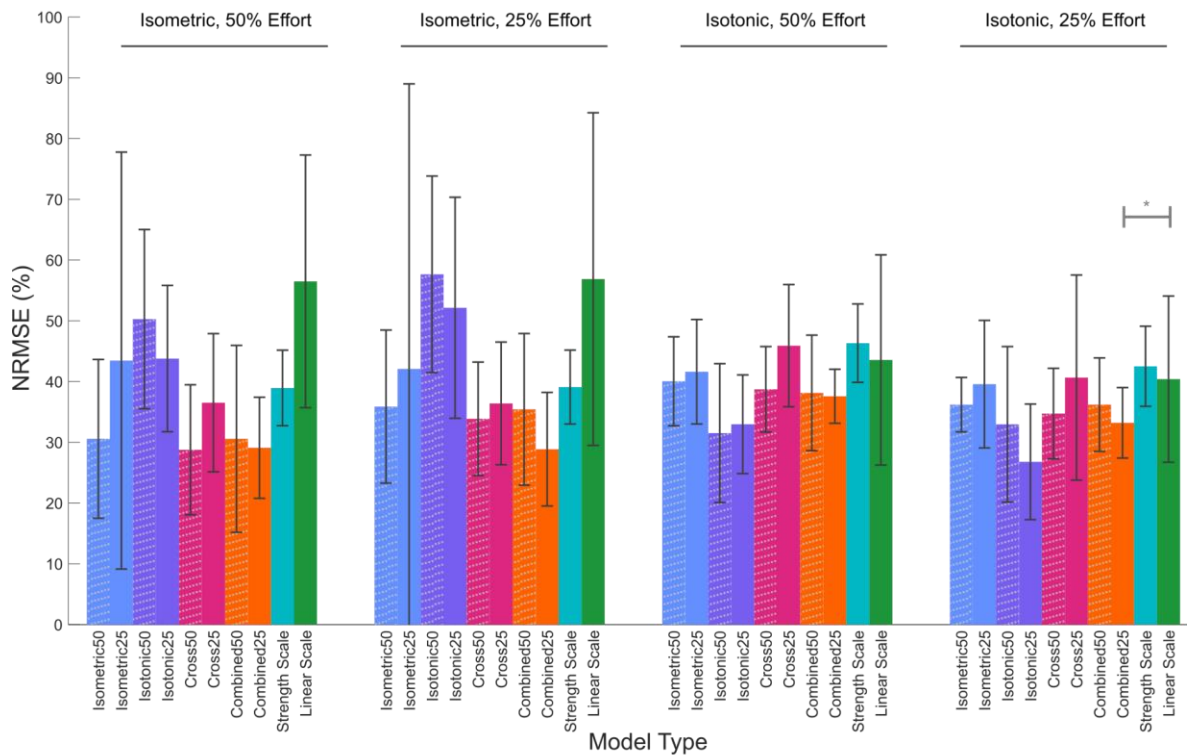


**Figure 3.4** Normalized root mean squared error (NRMSE) for each optimized and control model for each evaluation case. These bars and error bars represent the mean and standard deviation of the NRMSE over all study participants.

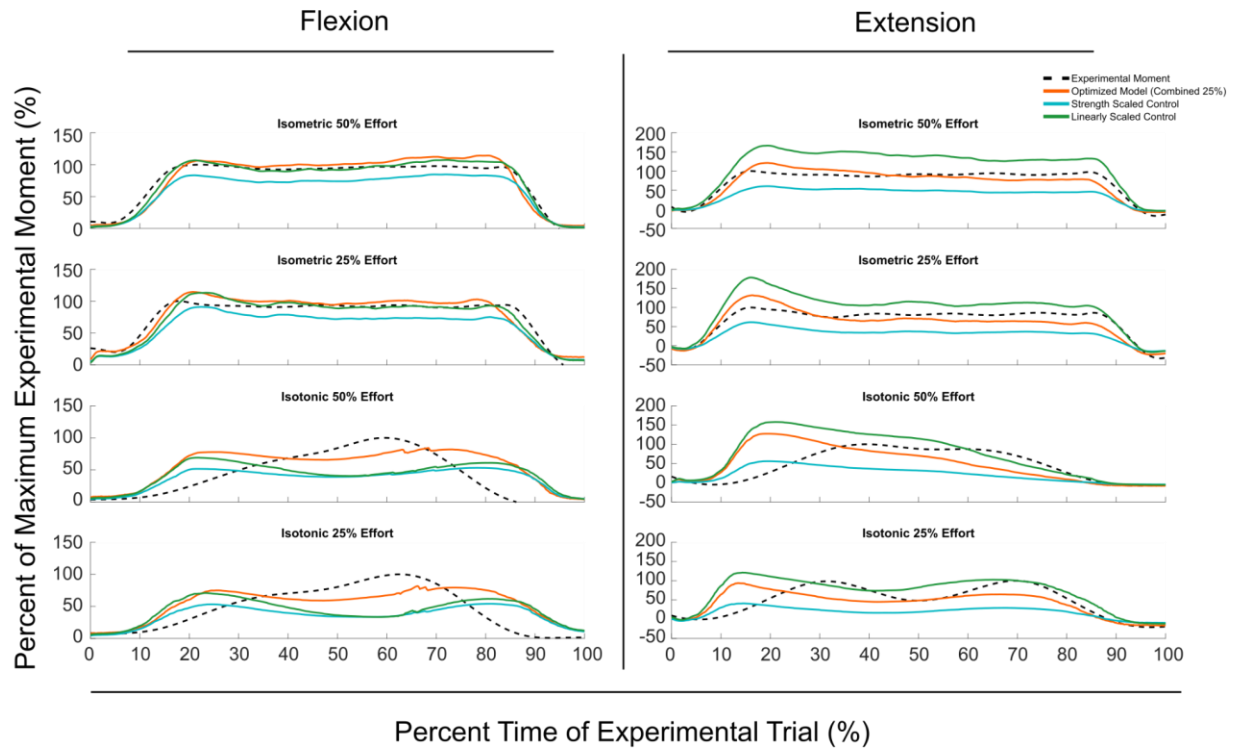
The repeated measures ANOVA indicated main effects of model types, evaluation types, effort levels, and interactions between evaluation type and model type, as well as between evaluation type and effort level ( $p < 0.05$ ; Table 3.4). Pairwise comparisons indicated the primary differences in NRMSE arose for the combined 25% effort model compared to the linear scaled control ( $p = 0.050$ ) when evaluated using the isotonic 25% effort trials. No other significant pairwise effects were observed for any other model case.

Table 3.3: NRMSE Evaluation ANOVA Results

<b>Comparison Factor(s)</b>	<b>F-statistic, p-value</b>
Model Type	<b>3.07, (0.03)</b>
Evaluation Type	<b>3.82, (0.02)</b>
Effort Level	<b>82.71, (&lt;0.001)</b>
Model Type x Evaluation Type	<b>78.21, (&lt;0.001*)</b>
Model Type x Effort Level	<b>79.39, (&lt;0.001*)</b>
Evaluation Type x Effort Level	<b>147.86, (&lt;0.001*)</b>

Table 3.4: Pearson's Correlation Coefficient Evaluation ANOVA Results

<b>Comparison Factor(s)</b>	<b>F-statistic, p-value</b>
Model Type	<b>2.07, 0.041</b>
Evaluation Type	<b>6.45, 0.002*</b>
Effort Level	<b>1615.30, &lt;0.001*</b>
Model Type x Evaluation Type	<b>430.44, &lt;0.001*</b>
Model Type x Effort Level	<b>381.92, &lt;0.001*</b>
Evaluation Type x Effort Level	<b>654.56, &lt;0.001*</b>



**Figure 3.5** Representative evaluation moment data of a study participant showing the moment generation of an optimized model case trained using the combined 25% effort data set in comparison to the two control models. Flexion trials are shown on the left side of the figure, while extension trials are shown on the right side of the figure. All data is scaled based on the maximum absolute moment generated during the experimental trial for each motion and effort level.

## Discussion

This work evaluated the effect of choice of training data set on the performance of personalized MSK models in comparison to existing scaling methods. Within the types of personalized models generated, optimization of the wrist flexors and extensors generally yielded MSK models that had a lower NRMSE on average compared to models scaled using traditional linear length scaling or simple strength scaling. The combined 25% effort case had the lowest overall NRMSE, while the isotonic 25% effort case had a marginally higher average Pearson's correlation coefficient in comparison to the other optimized model cases. When examined together the NRMSE and Pearson's correlation conducted here suggest that a combined data set consisting of both static and dynamic motion under light loading conditions may yield a somewhat more effective personalized model of the wrist in comparison to the control models. This is shown in the performance of representative cases in comparison to the control models (Figure 3.5), where for select cases, optimization is able to improve upon the controls.

However, while there were improvements in average performance using an optimized model, there were large standard deviations observed for each optimization case and generally non-significant pairwise differences between optimized cases and the control models. This suggests that while it is possible that joint-dynamics informed optimization may yield personalized MSK models that could be an improvement over simple strength scaled or linear scaled models, the statistical power may be too low given the sample size in this study to elicit specific pairwise differences that demonstrate this generally outside of select cases. A post-hoc power analysis performed using GPower (Faul et al., 2007), evaluated the differences in the mean absolute error between the optimized model trained on the combined 25% effort data set, and the linearly scaled model revealed an achieved statistical power of 0.67, with an effect size

calculated according to a Cohen's  $d$  parameter of 0.72. To achieve a larger statistical power of 0.8, a minimum sample size of 25 is needed. Examining the representative case (Figure 3.5), the overall differences between the optimized model and the controls were not very large. This may be due to linear scaling already capturing length or geometry dependent parameters close to the initial generic model, and the strength profiles of the individuals sampled in this study may not be substantially different from the generic model, as shown by the lack of significant differences in performance between the strength-scaled control and the linearly-scaled control models (Figure 3.4).

Each participant was able bodied with no history of wrist injury, and without any other outstanding factors that may result in significant differences between individuals. Previous work investigating wrist flexion strength has noted substantial differences in strength between individuals with chronic conditions such as arthritis or stroke, which reduce functional capacity, while individuals engaged in strenuous physical activity, such as boxing or rock climbing may have substantially increased wrist functional ability (Almkvist Muren et al., 2008; Goislard de Monsabert et al., 2017). Thus, recruitment of a larger pool of participants with a variety of levels of hand and wrist function, rather than a relatively small sample of healthy young adults, may elicit greater differences between the optimized and control models.

Future work should examine broader populations, including individuals both with and without a history of wrist injury, and individuals with outstanding factors to determine if our optimization approach is sensitive to these conditions. Additionally, as this study only examined a single degree of freedom, inclusion of compound motions and the addition of a minimal-effort kinematic only case may elicit more information for individual muscles, as well as enable more direct comparisons to previous studies.

Overall, this study represents one of the first systematic investigations into the inclusion of joint dynamics into the personalization of wrist MSK models, and the influence of experimental movement types and effort levels on the resulting model performance. While improvements using joint dynamics-informed optimization are modest, our results suggest that simple linear scaling is sufficient to predict task performance in healthy populations, and computationally intensive optimization for these groups may not be necessary. Importantly however, this work establishes an optimization and evaluation method that can be expanded to other joints in the upper limb, and provides a foundation for determining when sophistication in model personalization is necessary, such as potentially in populations that are substantially different from baseline, and when simpler approaches are more applicable.

## CHAPTER 4

### **In vivo ultrasound assessment of computationally predicted wrist muscle architecture**

(In preparation for the Journal of Biomechanics, 2026)

Christopher Jadelis, MS; Amy Adkins, PhD; Katherine R. Saul, PhD

#### **Abstract**

Muscle-specific architecture can inform assessment and rehabilitation for neuromuscular injuries and deformities (Adkins et al., 2021; Gao and Zhang, 2008; Kainz et al., 2021; Xu et al., 2025). However, measuring these features directly is often impractical. Indirect assessment using personalized computational musculoskeletal (MSK) models provides a potential alternative to estimate muscle-specific characteristics. However, current personalized modeling approaches have not assessed the physiological relevance of predicted muscle parameters, and instead focus on accuracy of endpoint predictions of task performance such as kinematics or moment production (Berman et al., 2023b; Hammond et al., 2025b; Pizzolato et al., 2015). Thus, it is unknown whether these models that successfully predict functional performance also reflect an individual's underlying architecture. To address this, we examined how well personalized MSK models, developed using optimization tools and conventional scaling methods, predict muscle architectural parameters (muscle length, tendon length, and maximum isometric force) as measured or estimated using in vivo ultrasound for the extensor carpi radialis brevis (ECRB), extensor carpi ulnaris (ECU), and flexor carpi radialis (FCR). We found that optimization, simple geometric scaling, and linear strength scaling captured trends in muscle belly and tendon length, with significant, moderate correlations ( $r > 0.5$ ,  $p < 0.05$ ) and limited prediction bias; however, only optimization-informed MSK models had significant correlations for maximum isometric force. Additionally, the limits of agreement for each parameter were large. These

suggest that personalized MSK models capture relative differences in muscle architecture across individuals and muscles, with optimization enabling greater insight over conventional scaling, but that absolute accuracy of predicted parameters remains inconsistent.

## **Introduction**

Understanding how individual muscles contribute to joint function during daily activities is of interest especially following neurologic injuries and developmental disorders such as stroke and cerebral palsy (Adkins et al., 2021; Gao and Zhang, 2008; Kainz et al., 2021; Xu et al., 2025). Gaining insights into the functional role of specific muscles in clinical populations may hold future promise for advancing rehabilitation regimens and the development of wearable robotics and assistive devices (Beckwée et al., 2021; Ghassemi and Kamper, 2021b; Hong et al., 2021). Currently available measurement techniques, such as surface electromyography (sEMG), are powerful tools that can discern relative muscle effort and inform how muscles behave together, but are unable to reveal anatomical muscle properties that determine a muscle's mechanical function. Aspects of muscle structure can be evaluated in vivo using imaging techniques such as ultrasound or magnetic resonance imaging (MRI) (Kainz et al., 2021; Saul et al., 2015) including direct measurement of muscle volume, fascicle length, cross sectional area, moment arm, and muscle belly and tendon length (Adkins et al., 2020; Scheys et al., 2008a). However, these imaging techniques require expert image acquisition and analysis to extract these values, can be time consuming and expensive and usually are unable to directly measure muscles during functional tasks.

Computational musculoskeletal (MSK) modeling provides an indirect method for estimating muscle characteristics and function. Simulation approaches can augment information derived from imaging methods by estimating muscle behavior during complex movements that

offer insight into a person's functional ability, such as fiber and tendon excursion, muscle power, and metabolic cost (McCain et al., 2021). When personalized measures of underlying muscle architecture and geometry are not available to inform such models, indirect prediction may be desirable using optimization or machine learning techniques (Berman et al., 2023b; Hammond et al., 2025b; Pizzolato et al., 2015). Current MSK models, such as those implemented in popular simulation platforms like OpenSim (Delp et al., 2007), typically rely on a combination of cadaveric and limited in vivo data to inform generic MSK models useful for general simulation (Holzbaur et al., 2005; McFarland et al., 2022; Rajagopal et al., 2016). To individualize these models, recent studies using indirect numeric optimization methods informed by functional task performance have successfully demonstrated the reproduction of joint torques in lower and upper limb MSK models, such as in the knee and wrist joints (Berman et al., 2023b; Hammond et al., 2025b; Han et al., 2025; Pizzolato et al., 2015).

However, while these predictive models can effectively reproduce experimental endpoints such as joint kinematics and torques, there is typically no evaluation of whether the predicted MSK parameters driving these personalized models correspond to their physiological counterparts. Some prior work has explored the validity of MSK model predictions such as fiber or tendon excursion of personalized MSK models in which the underlying muscle parameters or muscle paths are defined using direct measurements taken during intraoperative measurements (e.g. muscle fiber lengths and maximum isometric force) or three dimensional ultrasound (e.g. muscle paths) (Guenanten et al., 2024; Persad et al., 2023, 2021; Sartori et al., 2017). However, limited work has investigated the validity of MSK model muscle parameters produced by optimization-informed MSK models that do not incorporate directly measured architectural parameters.

To address these limitations, the objective of this work is to evaluate the physiological relevance of personalized MSK parameters derived via numeric optimization and linear scaling methods using ultrasound. Specifically, we estimated wrist MSK parameters using both a previously developed optimization tool (Chapter 3) and simple linear scaling methods and evaluated the physiological relevance of the parameters using direct in vivo measurements of related muscle structures. We generated model-predicted estimates of muscle length, tendon length, and maximum isometric force and compared with experimentally measured architectural parameters of the wrist flexor and extensor muscles using ultrasound in two wrist flexion postures. These experimental measures include muscle belly length, external tendon length, and estimates of muscle belly cross sectional area.

## **Methods**

### **Experimental Data Collection**

Five able-bodied participants (3 female and 2 male) with no history of wrist injury were recruited for this study, including three returning participants from (Chapters 2 and 3). Participants signed a consent form following a protocol approved by the North Carolina State University Institutional Review Board (IRB protocol number 5493). Strength and sEMG data were collected following the experimental protocol described in (Chapter 2). These were used to inform an optimization method and MSK model personalization described in (Chapter 3) that is used in this study, with all personalized MSK model types described in (Chapter 3) generated for each participant

Ultrasound imaging was performed to obtain physical measurements of the extensor carpi radialis brevis (ECRB), extensor carpi ulnaris (ECU), and the flexor carpi radialis (FCR) muscles. Images were collected using a Chison ECO 3 ultrasound system (Chison Medical

Technologies, Bellevue WA), equipped with an L7m-a linear probe operating with a chosen frequency of 7.5 MHz. The 3D position of the probe was recorded using eight Kestrel motion capture cameras (Motion Analysis, Rohnert Park, CA) tracking a custom motion capture marker attachment. Marker coordinates were post-processed in Motion Analysis Cortex, and a local coordinate system was defined with the origin at the center of the probe transducer surface to determine the distances between each image location. Motion capture markers were also placed on each participant at specific anatomical landmarks including at the shoulder closest to the humeral head, the lateral epicondyle of the humerus, and the styloid process of the radius and ulna (Figure 4.1). These markers were used to determine elbow flexion angle during each image capture sequence.

Transverse B-mode images were collected along the length of each muscle at four locations including the muscle origin, the muscle belly, the start of the external tendon, and the insertion point of each muscle. Images were collected in two wrist postures per muscle. All muscles were imaged in a neutral  $0^\circ$  wrist flexion posture; extensor muscles were also imaged in  $-30^\circ$  extension (flexion positive) and the FCR was imaged in  $+30^\circ$  flexion (Figure 4.1).

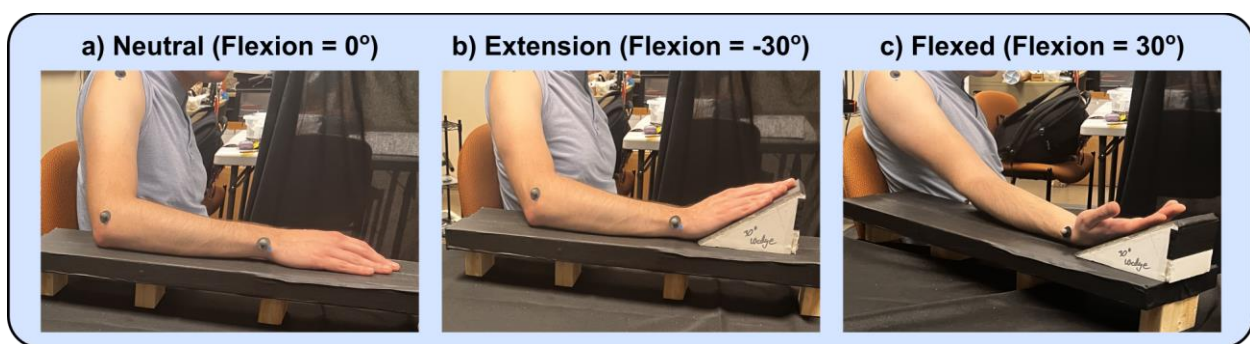


**Figure 4.1** Experimental postures and motion capture marker locations during ultrasound imaging. Motion capture markers are placed at anatomical landmarks to assess elbow flexion posture to compensate for changes in arm posture during each imaging session.

In each posture, anatomical muscle characteristics were measured. Muscle belly length was defined as the distance between the muscle origin and start of the external tendon. External tendon length was defined as the distance between the start of the external tendon and the muscle insertion point. Muscle cross sectional area was defined as the approximate cross-sectional area of the muscle when imaged with the ultrasound probe positioned above and perpendicular to the muscle belly. Muscle cross sectional areas were determined by processing the muscle belly cross sectional images (Figure 4.2) using the measurement tool in the Fiji distribution of ImageJ (Schindelin et al., 2012).

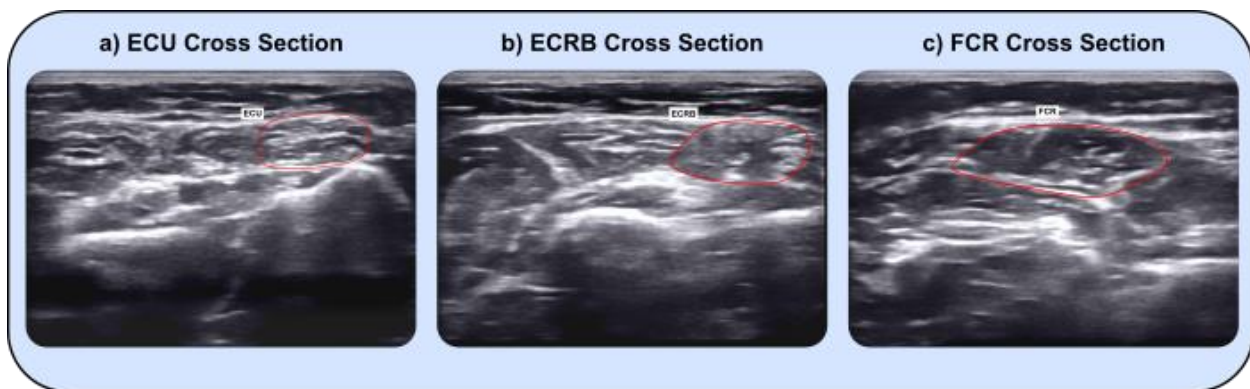


**Figure 4.2** Representative images of anatomical cross-sectional areas of the extensor carpi ulnaris a), the extensor carpi radialis brevis b), and the flexor carpi radialis c) from a single participant.

### **MSK Model and Optimization Tool and Equilibrium Simulations**

A previously developed wrist MSK model (McFarland et al., 2022) and optimization tool (Chapter 3) were selected for use in this study. To evaluate the parameters identified by the optimization tool, eight optimized model cases and two control cases were generated for each participant. The optimized model cases were trained using different combinations of the movement and relative effort data described in (Chapter 3). For comparison, two additional models scaled using standard non-optimization-based techniques were used as a control: linearly scaling and simple strength scaling. The linearly scaled model multiplied the generic optimal

fiber length and tendon slack length parameters by a linear scaling factor to match participant anthropometry using the ScaleTool from OpenSim. The simple strength scaled model also linearly scales optimal fiber length and tendon slack length with ScaleTool, while also altering maximum isometric force of each muscle such that the total joint torque produced by each muscle matches the experimental joint torque recorded during a maximum voluntary contraction (MVC) trial in the MVC experimental posture according to the methods presented in (McFarland et al., 2019). The list of optimized and control model cases are summarized in (Table 4.1). To replicate experimental conditions and extract predicted muscle and tendon lengths in the experimental postures, equilibrium simulations were performed using the OpenSim application programming interface within MATLAB 2023b (The Mathworks, Natick, MA). Each simulation was performed by setting the model elbow flexion, forearm supination (approximated as 90° for the extensor muscles, and -90° for the flexor muscles), and wrist flexion postures to match experimental conditions. Each muscle was initialized and equilibrated with a minimal muscle activation of 1% to approximate resting muscle activations during the imaging protocol. The estimated muscle fiber length and tendon length in the simulated test postures for muscle in each model case were used for analysis. The optimized maximum isometric muscle force parameter for each muscle in each model case was also used for analysis.

Table 4.1: Optimization and Control Model Case Data Types (Chapter 3)

<b>Data Type Used To Inform Muscle Parameters</b>		
<b><i>Optimized Model Case</i></b>	<b><i>Tendon Slack Length, Optimal Fiber Length (Contraction Type, Effort Level)</i></b>	<b><i>Maximum Isometric Force (Contraction Type, Effort Level)</i></b>
Isometric 50%	Isometric, 50%	Isometric, 50%
Isometric 25%	Isometric, 25%	Isometric, 25%
Isotonic 50%	Isotonic, 50%	Isotonic, 50%
Isotonic 25%	Isotonic 25%	Isotonic, 25%
Cross 50%	Isotonic, 50%	Isometric, 50%
Cross 25%	Isotonic, 25%	Isometric, 25%

Combined 50%	Isometric and Isotonic, 50%	Isometric and Isotonic, 25%
Combined 25%	Isometric and Isotonic, 25%	Isometric and Isotonic, 25%
<b><i>Control Model Cases</i></b>		
Linearly Scaled	Participant Anthropometry (scale factors)	N/A
Strength Scaled	Participant Anthropometry (scale factors)	Participant MVC Moment
<b>Statistical analysis</b>		

A linear regression and Pearson's correlation analysis were conducted for each optimized and control model case to determine if linear relationships exist between model estimated parameters and the corresponding measured muscle parameters. Given the exploratory nature of the study, all participants and muscles were analyzed in a combined dataset to increase the power of the analysis. Simulation estimates of muscle fiber length were compared to muscle belly length, tendon length was compared to external tendon length, and maximum isometric force was related to muscle belly cross sectional area.

A Tukey mean difference analysis was used to report simulation prediction bias and the limits of agreement of simulation estimates with ultrasound measurements. However, because the simulation estimates and ultrasound measurements are not directly relatable, we converted the estimates and measurements to allow more appropriate comparison. Specifically, the simulated muscle fiber lengths were converted to approximate muscle belly lengths using cadaveric muscle fiber length to muscle belly length ratios reported in (Lieber et al., 1990). Ultrasound external tendon lengths were converted to total tendon lengths using a ratio of the external tendon length to total tendon length for each muscle reported in (Loren and Lieber, 1995). Ultrasound muscle cross sectional areas were converted to estimated maximum tetanic tensions by multiplying the muscle belly cross sectional areas by specific tension ( $50.8 \text{ N/cm}^2$ ) as suggested for the muscles of the forearm in (Jacobson et al., 1992; Saul et al., 2015) for comparison to optimization-predicted maximum isometric force of each muscle. This approach was chosen as the expected pennation angle of each wrist muscle is small (Lieber et al., 1990),

and thus the muscle belly cross sectional area is approximately equivalent to the physiologic cross sectional area in this case. These converted measures are used to report the mean difference between simulation estimates and ultrasound measurements, as well as the limits of agreement of these measures, defined as 1.96 times the standard deviation of the differences between simulation estimates and ultrasound measurements (Cleveland, 1993).

## **Results**

### **MSK Model Pearson's Correlations**

Muscle parameters predicted by the optimized models were generally well correlated with experimentally measured values. For both muscle belly and tendon length, all optimized and control model cases had significant linear relationships between simulation-predicted and measured muscle parameters (Table 4.2), with Pearson's correlation coefficients for all models greater than 0.50 and 0.67 for muscle belly length and tendon length, respectively. Maximum isometric force was not as well correlated, with only three of the optimized model cases and neither of the control models having significant correlations (Table 4.2). Of the optimized cases with significant correlations for all three muscle parameters, the isotonic 50% effort case had the highest average Pearson's correlation (mean  $r = 0.67$ ), indicating a moderately strong linear relationship for all muscle parameters. This optimized model case is shown as a representative case (Figure 4.3; row 1) for comparison with the two control models (Figure 4.3; rows 2 and 3).

Table 4.2: MSK Model Pearson's Correlation Coefficients

<i>Muscle Parameter Correlation</i>			
<i>Optimized Model Case</i>	<i>Muscle Fiber to Muscle Belly Length (r, p-value)</i>	<i>Tendon Length to External Tendon Length (r, p-value)</i>	<i>Maximum Isometric Force to Muscle Cross Sectional Area (r, p-value)</i>
Isometric, 50% Effort	0.71, (<0.001*)	0.76, (<0.001*)	0.27, (0.155)
Isometric, 25% Effort	<b>0.80, (&lt;0.001*)</b>	<b>0.71, (&lt;0.001*)</b>	<b>0.40, (0.030*)</b>
Isotonic, 50% Effort	<b>0.57, (&lt;0.001*)</b>	<b>0.76, (&lt;0.001*)</b>	<b>0.67, (&lt;0.001*)</b>
Isotonic, 25% Effort	0.56, (0.001*)	0.71, (<0.001*)	0.33, (0.077)
Cross, 50% Effort	<b>0.57, (0.001*)</b>	<b>0.76, (&lt;0.001*)</b>	<b>0.40, (0.023*)</b>
Cross, 25% Effort	0.56, (0.001*)	0.71, (<0.001*)	0.07, (0.700)
Combined, 50% Effort	0.67, (<0.001*)	0.69, (<0.001*)	0.34, (0.063)
Combined, 25% Effort	0.64, (<0.001*)	0.67, (<0.001*)	0.23, (0.214)
<i>Control Model Case</i>			
Strength-scaled	0.64, (<0.001*)	0.86, (<0.001*)	0.30, (0.110)
Linear scaled	0.64, (<0.001*)	0.86, (<0.001*)	0.14, (0.470)

Note: Bolded rows indicate models that had significant correlations for all three parameters

### MSK Model Mean Difference and Agreement

The mean difference for all model cases for simulation-estimated muscle fiber length and ultrasound measured muscle belly length was moderate (<3.2cm); the mean difference between estimated and measured tendon length was minimal (<3mm). These results suggest that prediction bias for these parameters is small (Table 4.3). However, the limits of agreement for both muscle belly length and tendon length are broad, with maximum individual differences between predicted and measured parameters of 11.7 cm and 13.4 cm for muscle belly and tendon length, respectively. This suggests that absolute prediction accuracy is low for these parameters. Prediction bias and limits of agreement for maximum isometric force were both larger, with a

maximum bias of 190.8 N for the optimized models that exhibited significant correlations between simulated and measured parameters. This suggests that for these models, a consistent pattern of over or under prediction is present for maximum isometric force, and that absolute prediction accuracy is low.

Table 4.3: MSK Model Mean Difference and Limits of Agreement

<i>Muscle Parameter Mean Difference Analysis</i>			
<i>Optimized Model Case</i>	<i>Muscle Belly Length (Mean Difference (cm), Agreement Limit (cm))</i>	<i>Tendon Length (Mean Difference (cm), Agreement Limit (cm))</i>	<i>Maximum Isometric Force (Mean Difference (N), Agreement Limit (N))</i>
<i>Isometric, 50% Effort</i>	2.4, (0.82)	0.3, (13.2)	151.0, (276.8)
<i>Isometric, 25% Effort</i>	1.5, (0.91)	0.1, (13.1)	252.9, (596.1)
<i>Isotonic, 50% Effort</i>	3.0, (1.00)	0.1, (12.7)	152.2, (236.6)
<i>Isotonic, 25% Effort</i>	3.2, (1.17)	0.1, (13.0)	179.4, (389.3)
<i>Cross, 50% Effort</i>	3.0, (1.00)	0.1, (12.7)	177.6, (455.5)
<i>Cross, 25% Effort</i>	3.2, (1.17)	0.1, (13.0)	131.4, (451.9)
<i>Combined, 50% Effort</i>	2.4, (0.88)	0.4, (13.4)	153.7, (249.4)
<i>Combined, 25% Effort</i>	2.4, (0.88)	0.3, (13.4)	201.9, (317.1)
<b><i>Control Model Case</i></b>			
<i>Strength-scaled</i>	3.2, (0.93)	0.1, (13.1)	26.3, (86.6)
<i>Linear scaled</i>	3.2, (0.93)	0.1, (13.1)	184.2, (173.3)

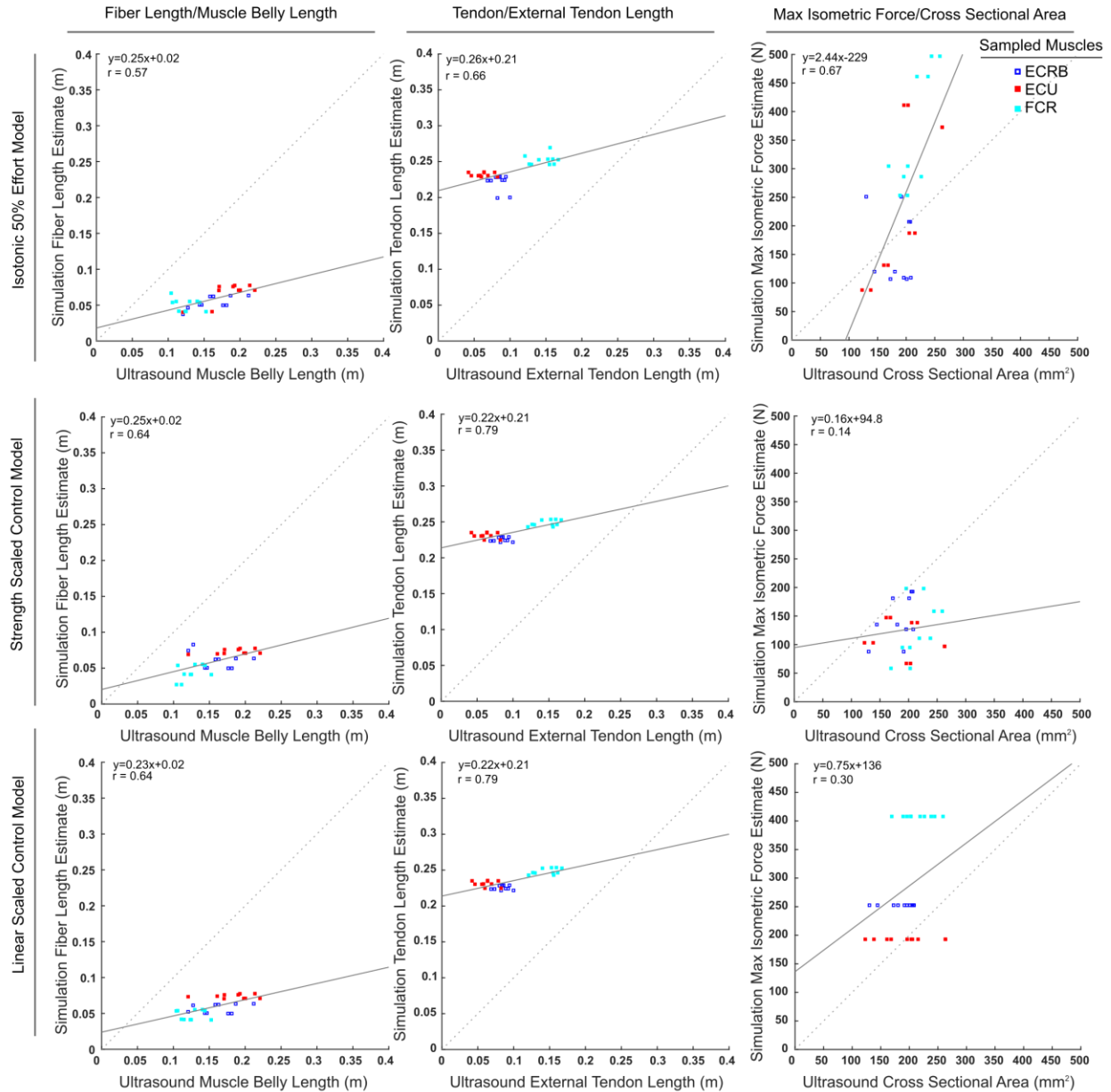


**Figure 4.3** Representative optimized model (row 1) corresponding to the isotonic 50% effort case (Table 4.1), and the two control model cases (rows 2 and 3) showing linear correlations between ultrasound recorded measurements and simulation estimates. These estimates include correlations between simulated fiber length and measured muscle belly length (column 1), simulated tendon length and measured external tendon length (column 2), and simulation-estimated maximum isometric force and measured muscle belly cross-sectional area (column 3).

## Discussion

This work provides new insight into the utility of model personalization for correlation of simulated MSK model parameters with in vivo muscle architecture.

Of the muscle architectural parameters examined here, muscle belly length and tendon length exhibited significant and moderately strong positive correlations between simulated muscle parameters and ultrasound measurements for all optimized and control model cases. The isotonic 50% effort model performed modestly better than all other models. This work supports that any of the models examined here were capable of capturing relative changes in muscle length and tendon length, with optimization offering modest benefits in comparison to conventional scaling. However, while the systemic prediction bias for these two parameters was relatively small for all cases, the limits of agreement are substantial, suggesting that absolute prediction accuracy was low regardless of model. When examining only muscle belly length and tendon length, model personalization using numeric optimization-informed approaches may not improve performance over conventional scaling approaches with regard to detection of length-dependent muscle architectural differences between healthy individuals. However, poor absolute prediction accuracy makes direct implementation of MSK models as an alternative to imaging methods currently impractical when absolute magnitude of architectural parameters are required. However, this observation should be considered in light of the limited ability to directly map from measured to simulated values. For example, the difficulty inherent in applying ultrasound imaging to measurement of muscle internal tendons and accurate measurement of muscle fiber length required conversion of direct measurements to ultrasound-derived quantities using mean architectural ratios previously reported in the literature based on cadaveric dissection (Lieber et al., 1990; Loren and Lieber, 1995). The variation in these reported mean ratios was minimal -

with a variation of  $<0.04$  for fiber length to muscle belly length and  $<8.7\text{mm}$  for external tendon to total tendon length (Lieber et al., 1990; Loren and Lieber, 1995) but these original ratios were reported for a small sample of cadaveric specimens, and thus may not be applicable to the participant group recruited for this study or reflect the breadth of variability present in the general population.

While length dependent parameters were well correlated to measured parameters for all models examined here, maximum isometric force was only well captured by the optimization-informed MSK models; only three of the optimized cases had significant ( $p < 0.05$ ) and moderately strong correlations, while neither of the control cases had significant correlations. The isotonic 50% effort case had the strongest correlation, and was able to capture a linear relationship between the ultrasound-measured muscle cross sectional area and simulation-predicted maximum isometric force. This indicates that while length dependent parameters may be well captured by existing scaling methods, optimization informed approaches may be necessary to sufficiently correlate with other muscle parameters. However, similar to muscle belly and tendon length, the systemic bias and limits of agreement for maximum isometric force imply that this approach may not be sufficient when absolute magnitudes of architectural parameters are needed.

The improved performance of optimization-informed approaches for maximum isometric force prediction over simpler scaling methods may be due to the limitations of the control models. For example, with linear scaling, maximum isometric force is not changed from nominal values. The strength-scaled control model does scale maximum isometric force; however, this scaling approach assumes a single scaling factor for each muscle group to maintain the relative muscle volume distribution. Thus, this method is unable to capture any muscle-specific variation

from the generic MSK model, while optimization-informed models are able to allow muscle-specific variations across individuals.

These findings are in line with previous studies examining muscle architectural parameter prediction accuracy, where personalization using directly measured fiber lengths from intraoperative measurements to inform an MSK model was able to reduce MSK prediction error between experimentally observed and MSK predicted fiber lengths and passive force production in a human gracilis muscle measured in four different postures (Persad et al., 2023). However, substantial prediction errors between MSK predicted and experimentally measured fiber lengths and passive force remain, as high as 20% and 37% respectively, preventing direct application of simulation predicted measurements in a clinical environment as a surrogate for imaging techniques. However, absent imaging methods for direct measurement of these architectural parameters, the correlations reported here provide new and novel utility in comparing an individual's muscle architecture relative to other groups, enabling the prediction of relative differences between individuals, and the potential for quantitative evaluation of muscle function for detection of muscle specific deficits. Quantification of muscle specific deficits may be of particular interest in determining the effectiveness of interventions over time for individuals with musculoskeletal injuries known to result in changes in muscle architecture, such as stroke injury. These architectural changes include abnormal reduction in muscle fiber length and sarcopenia, due to reduction in the number of serial sarcomeres in muscle fibers, reduction in muscle cross sectional area, and changes in composition of fiber type within a muscle (Adkins et al., 2021; Beckwée et al., 2021). Simple linear scaling from nominal values may not be appropriate for populations with these injuries, while optimization informed parameter correlation may be able to capture these changes.

While these correlations are promising, this study is ultimately exploratory and the sample size is small, which may contribute to the observed limits of agreement for all parameters. Additionally, as the population surveyed in this study were all healthy able-bodied individuals with no history of wrist injury, additional investigation with impaired or injured participants is necessary to conclusively determine the applicability of these correlation measures with injured groups. A post-hoc power analysis using GPower version 3.1.9.7 (Faul et al., 2007), using the correlation coefficient calculated for the isotonic 25% effort case to determine effect size ( $r = 0.64$ ), suggests an achieved statistical power of 42%. Future assessments with a minimum achieved power of 80% should include a minimum sample size of at least 11 participants.

Overall, this study demonstrates that personalized MSK models are able to capture trends in muscle architectural parameters, with the trends providing utility in person-specific comparison to larger population groups. This study also identifies specific types of optimization-informed personalized MSK models that may reveal useful insights that are not available using relatively simple scaling methods.

## **CHAPTER 5: Conclusions**

### **Contributions**

This dissertation presents novel investigations that improve our understanding of experimental task selection strategies for use in personalization of computational musculoskeletal models, and the potential applications for these models in clinical environments. The studies conducted here have several important contributions. In Chapter 2 this work evaluated the effect of different experimental movement types and impact of participant relative effort level on the sensitivity of individual musculoskeletal parameters to the response of a wrist musculoskeletal model. While previous work has conducted sensitivity studies investigating the relative importance of individual muscle parameters for their inclusion in further optimization of MSK models (Diaz et al., 2023; Han et al., 2025; Hinson et al., 2022), this is to our knowledge the first study that systematically examines multiple experimental types and participant effort levels, and examines the impact that these specific experiments have on the response of an MSK model. This research specifically identifies the relationship between the influence of specific muscle parameters on MSK model response, and the experimental data used for simulation, enabling specific recommendations to be made for data collection procedures for MSK model personalization. We specifically identified that muscle parameters such as tendon slack length and optimal fiber length are most influential to model response during dynamic motion, represented in this work as isotonic muscle contractions, whereas maximum isometric force is equally influential under all tested experimental conditions. Additionally, contrary to our initial hypothesis, we identify that increasing participant relative effort during experimental trials does not yield more information about specific muscle parameters, with light effort tasks encompassing 25% of a participant's maximum effort being equivalent to tasks at 50% of a

participant's maximum effort. The results of this study provide insight into the suitability of specific experimental movements to inform specific muscle parameters in optimization and may aid in the standardization of experimental data collection procedures for the wrist.

In Chapter 3, I expand on the findings presented in Chapter 2 by utilizing the experimental movement type and effort level data to investigate the suitability of these for the creation of joint dynamics informed personalized MSK models. In this study, I evaluated the suitability of different experimental movement types and participant effort levels, and combinations of these for the creation of accurate personalized MSK models that are performant over a wide range of tasks. Additionally, we compared these personalized models to relatively simple linearly scaled MSK models to determine the appropriateness of optimization for personalization. This study, similar to the study in Chapter 2, is the first of its kind that directly implements experimentally measured joint torques in the personalization of a wrist MSK model. Contrary to our initial hypothesis, we identified that for healthy able-bodied participants, computationally expensive optimization may not be necessary to produce personalized MSK models that capture functional movement, and that for participants with strength profiles similar to the nominal model, simple linear scaling is an effective personalization method. Of the optimized models, however, we demonstrated that a combination of movement types regardless of participant effort level may yield a more robust personalized MSK model in comparison to optimization informed by singular movement types. Importantly, this study identifies participant groups that may not benefit from optimization, while providing insight into future work with other populations that may benefit from more advanced approaches.

Lastly, in Chapter 4 I investigated the clinical relevance of the parameter predictions in Chapter 3, by correlating the personalized MSK model predictions of muscle architecture with in

vivo experimental measurements. This study represents the first of its kind that examines how predicted MSK parameters in a wrist MSK model correlate with measured in vivo muscle architecture. Previous work has examined the accuracy of predicted MSK muscle behavior, such as muscle fiber length and passive stiffness when informed using direct intra-operative measurements or linear scaling; however, to our knowledge, this work is the first to examine optimization informed personalized MSK models specifically. We identified in this study that significant and positive correlations exist for muscle architectural parameters and predicted MSK parameters for muscle fiber length and tendon length, and that these correlations are consistent for both optimization informed models and linearly scaled MSK models. However, for muscle parameters not included in linear scaling such as maximum isometric force, optimization informed approaches are necessary to capture significant correlations between predicted and experimentally measured parameters. This result provides new insight into the clinical applicability of MSK models and hopefully will lead to improvements in clinical diagnostic procedures.

### **Applications**

The work presented in this dissertation has many potential future applications. We demonstrate the sensitivity of muscle parameters to different experimental task types and effort levels for use in optimization of MSK models of the wrist. These results can be used to effectively standardize the requirements for data collection in developing personalized MSK models and encourage the inclusion of light effort dynamic tasks to better inform parameters such as optimal fiber length and tendon slack length.

Additionally, the work presented in Chapter 3 for selection of training data for optimization informed personalization of MSK models demonstrates that for healthy able-bodied

participants, current linear scaling methods are already sufficient to capture functional capacity, identifying instances where optimization-based approaches are unnecessary. The optimization toolset developed as part of this work, however, does enable an optimization-based approach to determining parameters not associated with limb length, such as maximum isometric force, which may allow for determination of atypical functional capacity, such as observed in population groups with injuries or disabilities.

Lastly, the correlation of predicted MSK parameters with experimentally measured muscle architecture reveals clinical applications of personalized MSK models, with the potential to use optimization based MSK model personalization methods to identify specific muscle architectural differences between individual groups. This result may enable clinicians to capture muscle specific deficits, and track the improvement of these deficits over time, providing a useful quantitative metric for evaluating rehabilitative therapies.

## **Future Work**

### **Expansion to More Complex MSK Models**

In this dissertation I examined a wrist MSK model with a subset of five muscles and a single degree of freedom, additionally I examined two different movement types and participant effort levels. This research provides insight specific experimental procedures, optimization training data, and optimized models that can provide the basis for standardized measurement procedures and clinical correlation tools for measurement of functional capability and muscle specific deficits. However, as the wrist is a biarticular joint, with multiple muscles crossing it that have contributions to wrist flexion and wrist deviation, future studies expanding on this work may explore the sensitivity of muscle parameters to additional degrees of freedom, and the role of additional muscles in the function of the wrist. Additionally, as the wrist is a relatively

easily accessible joint for torque measurement, these methods may also be applied to the hand and fingers, examining muscles that cross not only the wrist, but also the metacarpophalangeal joints, to gain insight into the digits of the hand, and advance towards a full personalized model of both the wrist and the hand.

### **Inclusion of Clinical Populations**

Our research provides preliminary evidence that optimization informed personalized models may enable insight into muscle specific deficits based on correlations between predicted MSK parameters and experimentally measured muscle architecture. However, the population sampled in these studies was relatively small and composed of healthy able-bodied individuals. The tools and methods presented here could be used by a researcher to expand the dataset to include more individuals to gain confidence in these correlations and include populations with known muscle architectural differences either due to disease and injury, or those with exceptional functional capacity, such as high-performance athletes. The results of such a future study could provide further insight into muscle architectural changes because of injury conditions, as well as provide insight into athletic training to improve athlete performance.

### **Direct Comparison with Experimental Measurements**

We used ultrasonography to directly determine muscle architectural features of the participants sampled in these studies; however, due to the need for high resolution equipment and imaging expertise, the number of architectural features we were able to measure was limited. A future study that combines the motion capture apparatus used here, with more advanced ultrasound capabilities may enable direct capture of additional architectural features, such as muscle pennation angle and fascicle length using extended field of view ultrasonography.

## **Exploration of Population Based Constraints**

We conducted model personalization of a wrist MSK model, with parameter constraints informed by previous cadaver and in vivo studies. However, as these constraints are three standard deviations above and below the mean for limited populations, these constraint values may not be reflective of a general population. A parameter distribution derived from these preliminary optimized models may be used to inform future optimization studies and derive a set of distribution constraints that are better reflective of the general population.

## REFERENCES

- Adkins, A.N., Dewald, J.P.A., Garmirian, L.P., Nelson, C.M., Murray, W.M., 2021. Serial sarcomere number is substantially decreased within the paretic biceps brachii in individuals with chronic hemiparetic stroke. *Proc. Natl. Acad. Sci.* 118, e2008597118. <https://doi.org/10.1073/pnas.2008597118>
- Adkins, A.N., Murray, W.M., Adkins, A.N., Murray, W.M., 2020. Obtaining Quality Extended Field-of-View Ultrasound Images of Skeletal Muscle to Measure Muscle Fascicle Length. *J. Vis. Exp.* e61765. <https://doi.org/10.3791/61765>
- Akbas, T., Sulzer, J., 2019. Musculoskeletal simulation framework for impairment-based exoskeletal assistance post-stroke, in: 2019 IEEE 16th International Conference on Rehabilitation Robotics (ICORR). Presented at the 2019 IEEE 16th International Conference on Rehabilitation Robotics (ICORR), pp. 1185–1190. <https://doi.org/10.1109/ICORR.2019.8779564>
- Almkvist Muren, M., Hütler, M., Hooper, J., 2008. Functional Capacity and Health-Related Quality of Life in Individuals Post Stroke. *Top. Stroke Rehabil.* 15, 51–58. <https://doi.org/10.1310/tsr1501-51>
- Ao, D., Li, G., Shourijeh, M.S., Patten, C., Fregly, B.J., 2023. EMG-Driven Musculoskeletal Model Calibration With Wrapping Surface Personalization. *IEEE Trans. Neural Syst. Rehabil. Eng. Publ. IEEE Eng. Med. Biol. Soc.* 31, 4235–4244. <https://doi.org/10.1109/TNSRE.2023.3323516>
- Barry, A.J., Kamper, D.G., Stoykov, M.E., Triandafilou, K., Roth, E., 2022. Characteristics of the severely impaired hand in survivors of stroke with chronic impairments. *Top. Stroke Rehabil.* 29, 181–191. <https://doi.org/10.1080/10749357.2021.1894660>
- Beckwée, D., Lefeber, N., Bautmans, I., Cuypers, L., De Keersmaecker, E., De Raedt, S., Kerckhofs, E., Nagels, G., Njemini, R., Perkisas, S., Scheys, E., Swinnen, E., 2021. Muscle changes after stroke and their impact on recovery: time for a paradigm shift? Review and commentary. *Top. Stroke Rehabil.* 28, 104–111. <https://doi.org/10.1080/10749357.2020.1783916>
- Bennett, K.J., Pizzolato, C., Martelli, S., Bahl, J.S., Sivakumar, A., Atkins, G.J., Solomon, L.B., Thewlis, D., 2022. EMG-Informed Neuromusculoskeletal Models Accurately Predict Knee Loading Measured Using Instrumented Implants. *IEEE Trans. Biomed. Eng.* 69, 2268–2275. <https://doi.org/10.1109/TBME.2022.3141067>
- Berman, J., Hinson, R., Lee, I.-C., Huang, H., 2023a. Harnessing Machine Learning and Physiological Knowledge for a Novel EMG-Based Neural-Machine Interface. *IEEE Trans. Biomed. Eng.* 70, 1125–1136. <https://doi.org/10.1109/TBME.2022.3210892>

- Berman, J., Hinson, R., Lee, I.-C., Huang, H., 2023b. Harnessing Machine Learning and Physiological Knowledge for a Novel EMG-Based Neural-Machine Interface. *IEEE Trans. Biomed. Eng.* 70, 1125–1136. <https://doi.org/10.1109/TBME.2022.3210892>
- Binder-Markey, B.I., Dewald, J.P.A., Murray, W.M., 2019. The Biomechanical Basis of the Claw Finger Deformity: A Computational Simulation Study. *J. Hand Surg.* 44, 751–761. <https://doi.org/10.1016/j.jhsa.2019.05.007>
- Cleveland, W.S., 1993. *Visualizing data*. At & T Bell Laboratories ; [Published by Hobart Press], Murray Hill, N.J., [Summit, N.J.].
- Conrad, M.O., Kamper, D.G., 2012. Isokinetic strength and power deficits in the hand following stroke. *Clin. Neurophysiol. Off. J. Int. Fed. Clin. Neurophysiol.* 123, 1200–1206. <https://doi.org/10.1016/j.clinph.2011.10.004>
- Crouch, D.L., Huang, H., 2016. Lumped-parameter electromyogram-driven musculoskeletal hand model: A potential platform for real-time prosthesis control. *J. Biomech.* 49, 3901–3907. <https://doi.org/10.1016/j.jbiomech.2016.10.035>
- Dalman, M., Liao, A., Saul, K.R., 2022. Evaluating anthropometric scaling of a generic adult model to represent pediatric shoulder strength. *J. Biomech.* 141, 111170. <https://doi.org/10.1016/j.jbiomech.2022.111170>
- Dang, M., Ramsaran, K.D., Street, M.E., Syed, S.N., Barclay-Goddard, R., Stratford, P.W., Miller, P.A., 2011. Estimating the Accuracy of the Chedoke–McMaster Stroke Assessment Predictive Equations for Stroke Rehabilitation. *Physiother. Can.* 63, 334–341. <https://doi.org/10.3138/ptc.2010-17>
- Delp, S.L., Anderson, F.C., Arnold, A.S., Loan, P., Habib, A., John, C.T., Guendelman, E., Thelen, D.G., 2007. OpenSim: Open-Source Software to Create and Analyze Dynamic Simulations of Movement. *IEEE Trans. Biomed. Eng.* 54, 1940–1950. <https://doi.org/10.1109/TBME.2007.901024>
- Diaz, M.T., Harley, J.B., Nichols, J.A., 2023. Sensitivity Analysis of Upper Limb Musculoskeletal Models During Isometric and Isokinetic Tasks. *J. Biomech. Eng.* 146. <https://doi.org/10.1115/1.4064056>
- Duruöz, M.T., 2014. *Hand Function: A Practical Guide to Assessment*. Springer Science & Business Media.
- Dwivedi, S.K., Ngeo, J., Shibata, T., 2020. Extraction of Nonlinear Synergies for Proportional and Simultaneous Estimation of Finger Kinematics. *IEEE Trans. Biomed. Eng.* 67, 2646–2658. <https://doi.org/10.1109/TBME.2020.2967154>

- Faber, G.S., Chang, C.-C., Kingma, I., Dennerlein, J.T., 2013. Estimating dynamic external hand forces during manual materials handling based on ground reaction forces and body segment accelerations. *J. Biomech.* 46, 2736–2740. <https://doi.org/10.1016/j.jbiomech.2013.07.030>
- Faul, F., Erdfelder, E., Lang, A.-G., Buchner, A., 2007. G\*Power 3: a flexible statistical power analysis program for the social, behavioral, and biomedical sciences. *Behav. Res. Methods* 39, 175–191. <https://doi.org/10.3758/bf03193146>
- Fregly, B.J., 2021. A Conceptual Blueprint for Making Neuromusculoskeletal Models Clinically Useful. *Appl. Sci.* 11, 2037. <https://doi.org/10.3390/app11052037>
- Fregly, B.J., Boninger, M.L., Reinkensmeyer, D.J., 2012. Personalized neuromusculoskeletal modeling to improve treatment of mobility impairments: a perspective from European research sites. *J. NeuroEngineering Rehabil.* 9, 18. <https://doi.org/10.1186/1743-0003-9-18>
- Gao, F., Zhang, L.-Q., 2008. Altered contractile properties of the gastrocnemius muscle poststroke. *J. Appl. Physiol.* 105, 1802–1808. <https://doi.org/10.1152/japplphysiol.90930.2008>
- Ghassemi, M., Kamper, D.G., 2022. The Hand After Stroke and SCI: Restoration of Function with Technology, in: Reinkensmeyer, D.J., Marchal-Crespo, L., Dietz, V. (Eds.), *Neurorehabilitation Technology*. Springer International Publishing, Cham, pp. 113–134. [https://doi.org/10.1007/978-3-031-08995-4\\_6](https://doi.org/10.1007/978-3-031-08995-4_6)
- Ghassemi, M., Kamper, D.G., 2021a. A Hand Exoskeleton for Stroke Survivors' Activities of Daily Life, in: 2021 43rd Annual International Conference of the IEEE Engineering in Medicine & Biology Society (EMBC). Presented at the 2021 43rd Annual International Conference of the IEEE Engineering in Medicine & Biology Society (EMBC), pp. 6734–6737. <https://doi.org/10.1109/EMBC46164.2021.9629805>
- Ghassemi, M., Kamper, D.G., 2021b. A Hand Exoskeleton for Stroke Survivors' Activities of Daily Life, in: 2021 43rd Annual International Conference of the IEEE Engineering in Medicine & Biology Society (EMBC). Presented at the 2021 43rd Annual International Conference of the IEEE Engineering in Medicine & Biology Society (EMBC), pp. 6734–6737. <https://doi.org/10.1109/EMBC46164.2021.9629805>
- Goislard De Monsabert, B., Edwards, D., Shah, D., Kedgley, A., 2018. Importance of Consistent Datasets in Musculoskeletal Modelling: A Study of the Hand and Wrist. *Ann. Biomed. Eng.* 46, 71–85. <https://doi.org/10.1007/s10439-017-1936-z>
- Goislard de Monsabert, B., Rao, G., Gay, A., Berton, E., Vigouroux, L., 2017. A scaling method to individualise muscle force capacities in musculoskeletal models of the hand and wrist using isometric strength measurements. *Med. Biol. Eng. Comput.* 55, 2227–2244. <https://doi.org/10.1007/s11517-017-1662-6>

- Guenanten, H., Retailleau, M., Dorel, S., Sarcher, A., Colloud, F., Nordez, A., 2024. Muscle-Tendon Unit Length Measurement Using 3D Ultrasound in Passive Conditions: OpenSim Validation and Development of Personalized Models. *Ann. Biomed. Eng.* 52, 997–1008. <https://doi.org/10.1007/s10439-023-03436-2>
- Hammond, C.V., Williams, S.T., Vega, M.M., Ao, D., Li, G., Salati, R.M., Pariser, K.M., Shourijeh, M.S., Habib, A.W., Patten, C., Fregly, B.J., 2025a. The Neuromusculoskeletal Modeling Pipeline: MATLAB-based model personalization and treatment optimization functionality for OpenSim. *J. NeuroEngineering Rehabil.* 22, 112. <https://doi.org/10.1186/s12984-025-01629-5>
- Hammond, C.V., Williams, S.T., Vega, M.M., Ao, D., Li, G., Salati, R.M., Pariser, K.M., Shourijeh, M.S., Habib, A.W., Patten, C., Fregly, B.J., 2025b. The Neuromusculoskeletal Modeling Pipeline: MATLAB-based model personalization and treatment optimization functionality for OpenSim. *J. NeuroEngineering Rehabil.* 22, 112. <https://doi.org/10.1186/s12984-025-01629-5>
- Hammond, C.V., Williams, S.T., Vega, M.M., Ao, D., Li, G., Salati, R.M., Pariser, K.M., Shourijeh, M.S., Habib, A.W., Patten, C., Fregly, B.J., 2025c. The Neuromusculoskeletal Modeling Pipeline: MATLAB-based model personalization and treatment optimization functionality for OpenSim. *J. Neuroengineering Rehabil.* 22, 112. <https://doi.org/10.1186/s12984-025-01629-5>
- Han, L., Cheng, L., Li, H., Zou, Y., Qin, S., Zhou, M., 2025. Hierarchical Optimization for Personalized Hand and Wrist Musculoskeletal Modeling and Motion Estimation. *IEEE Trans. Biomed. Eng.* 72, 454–465. <https://doi.org/10.1109/TBME.2024.3456235>
- Hill, A.V., 1938. The heat of shortening and the dynamic constants of muscle. *Proc. R. Soc. Lond. Ser. B - Biol. Sci.* 126, 136–195. <https://doi.org/10.1098/rspb.1938.0050>
- Hinson, R., Saul, K., Kamper, D., Huang, H., 2022. Sensitivity analysis guided improvement of an electromyogram-driven lumped parameter musculoskeletal hand model. *J. Biomech.* 141, 111200. <https://doi.org/10.1016/j.jbiomech.2022.111200>
- Holzbour, K.R.S., Delp, S.L., Gold, G.E., Murray, W.M., 2007. Moment-generating capacity of upper limb muscles in healthy adults. *J. Biomech.* 40, 2442–2449. <https://doi.org/10.1016/j.jbiomech.2006.11.013>
- Holzbour, K.R.S., Murray, W.M., Delp, S.L., 2005. A model of the upper extremity for simulating musculoskeletal surgery and analyzing neuromuscular control. *Ann. Biomed. Eng.* 33, 829–840. <https://doi.org/10.1007/s10439-005-3320-7>
- Hong, Y.N.G., Ballekere, A.N., Fregly, B.J., Roh, J., 2021. Are muscle synergies useful for stroke rehabilitation? *Curr. Opin. Biomed. Eng.* 19, 100315. <https://doi.org/10.1016/j.cobme.2021.100315>

- Jacobson, M.D., Raab, R., Fazeli, B.M., Abrams, R.A., Botte, M.J., Lieber, R.L., 1992. Architectural design of the human intrinsic hand muscles. *J. Hand Surg.* 17, 804–809. [https://doi.org/10.1016/0363-5023\(92\)90446-V](https://doi.org/10.1016/0363-5023(92)90446-V)
- Kainz, H., Wesseling, M., Jonkers, I., 2021. Generic scaled versus subject-specific models for the calculation of musculoskeletal loading in cerebral palsy gait: Effect of personalized musculoskeletal geometry outweighs the effect of personalized neural control. *Clin. Biomech.* 87, 105402. <https://doi.org/10.1016/j.clinbiomech.2021.105402>
- Lichtwark, G.A., Farris, D.J., Chen, X., Hodges, P.W., Delp, S.L., 2018. Microendoscopy reveals positive correlation in multiscale length changes and variable sarcomere lengths across different regions of human muscle. *J. Appl. Physiol.* 125, 1812–1820. <https://doi.org/10.1152/jappphysiol.00480.2018>
- Lieber, R.L., Fazeli, B.M., Botte, M.J., 1990. Architecture of selected wrist flexor and extensor muscles. *J. Hand Surg.* 15, 244–250. [https://doi.org/10.1016/0363-5023\(90\)90103-X](https://doi.org/10.1016/0363-5023(90)90103-X)
- Lieber, R.L., Jacobson, M.D., Fazeli, B.M., Abrams, R.A., Botte, M.J., 1992. Architecture of selected muscles of the arm and forearm: Anatomy and implications for tendon transfer. *J. Hand Surg.* 17, 787–798. [https://doi.org/10.1016/0363-5023\(92\)90444-T](https://doi.org/10.1016/0363-5023(92)90444-T)
- Loren, G.J., Lieber, R.L., 1995. Tendon biomechanical properties enhance human wrist muscle specialization. *J. Biomech.* 28, 791–799. [https://doi.org/10.1016/0021-9290\(94\)00137-S](https://doi.org/10.1016/0021-9290(94)00137-S)
- McCain, E.M., Berno, M.E., Libera, T.L., Lewek, M.D., Sawicki, G.S., Saul, K.R., 2021. Reduced joint motion supersedes asymmetry in explaining increased metabolic demand during walking with mechanical restriction. *J. Biomech.* 126, 110621. <https://doi.org/10.1016/j.jbiomech.2021.110621>
- McFarland, D.C., Binder-Markey, B.I., Nichols, J.A., Wohlman, S.J., de Bruin, M., M. Murray, W., 2022. A Musculoskeletal Model of the Hand and Wrist Capable of Simulating Functional Tasks. *IEEE Trans. Biomed. Eng.* 1–12. <https://doi.org/10.1109/TBME.2022.3217722>
- McFarland, D.C., McCain, E.M., Poppo, M.N., Saul, K.R., 2019. Spatial Dependency of Glenohumeral Joint Stability During Dynamic Unimanual and Bimanual Pushing and Pulling. *J. Biomech. Eng.* 141. <https://doi.org/10.1115/1.4043035>
- Millard, M., Uchida, T., Seth, A., Delp, S.L., 2013. Flexing Computational Muscle: Modeling and Simulation of Musculotendon Dynamics. *J. Biomech. Eng.* 135. <https://doi.org/10.1115/1.4023390>
- Morris, M.D., 1991. Factorial Sampling Plans for Preliminary Computational Experiments. *Technometrics* 33, 161–174. <https://doi.org/10.1080/00401706.1991.10484804>

- Persad, L.S., Ates, F., Shin, A.Y., Lieber, R.L., Kaufman, K.R., 2021. Measuring and modeling *in vivo* human gracilis muscle-tendon unit length. *J. Biomech.* 125, 110592. <https://doi.org/10.1016/j.jbiomech.2021.110592>
- Persad, L.S., Binder-Markey, B.I., Shin, A.Y., Lieber, R.L., Kaufman, K.R., 2023. American Society of Biomechanics Journal of Biomechanics Award 2022: Computer models do not accurately predict human muscle passive muscle force and fiber length: Evaluating subject-specific modeling impact on musculoskeletal model predictions. *J. Biomech.* 159, 111798. <https://doi.org/10.1016/j.jbiomech.2023.111798>
- Pianosì, F., Sarrazin, F., Wagener, T., 2015. A Matlab toolbox for Global Sensitivity Analysis. *Environ. Model. Softw.* 70, 80–85. <https://doi.org/10.1016/j.envsoft.2015.04.009>
- Pizzolato, C., Lloyd, D.G., Sartori, M., Ceseracciu, E., Besier, T.F., Fregly, B.J., Reggiani, M., 2015. CEINMS: A toolbox to investigate the influence of different neural control solutions on the prediction of muscle excitation and joint moments during dynamic motor tasks. *J. Biomech.* 48, 3929–3936. <https://doi.org/10.1016/j.jbiomech.2015.09.021>
- Rajagopal, A., Dembia, C.L., DeMers, M.S., Delp, D.D., Hicks, J.L., Delp, S.L., 2016. Full-Body Musculoskeletal Model for Muscle-Driven Simulation of Human Gait. *IEEE Trans. Biomed. Eng.* 63, 2068–2079. <https://doi.org/10.1109/TBME.2016.2586891>
- Rassier, D.E., 2017. Sarcomere mechanics in striated muscles: from molecules to sarcomeres to cells. *Am. J. Physiol.-Cell Physiol.* 313, C134–C145. <https://doi.org/10.1152/ajpcell.00050.2017>
- Riddle, M., MacDermid, J., Robinson, S., Szekeres, M., Ferreira, L., Lalone, E., 2020. Evaluation of individual finger forces during activities of daily living in healthy individuals and those with hand arthritis. *J. Hand Ther.* 33, 188–197. <https://doi.org/10.1016/j.jht.2020.04.002>
- Rook, J.W.A., Sartori, M., Refai, M.I., 2025. Toward Wearable Electromyography for Personalized Musculoskeletal Trunk Models Using an Inverse Synergy-Based Approach. *IEEE Trans. Med. Robot. Bionics* 7, 13–19. <https://doi.org/10.1109/TMRB.2024.3503900>
- Sacks, L., Yee, K., Huijbregts, M., Miller, P., Aggett, T., Salbach, N., 2010. Validation of the activity inventory of the Chedoke-McMaster stroke assessment and the clinical outcome variables scale to evaluate mobility in geriatric clients. *J. Rehabil. Med. Off. J. UEMS Eur. Board Phys. Rehabil. Med.* 42, 90–2. <https://doi.org/10.2340/16501977-0477>
- Sartori, M., Durandau, G., Došen, S., Farina, D., 2018. Robust simultaneous myoelectric control of multiple degrees of freedom in wrist-hand prostheses by real-time neuromusculoskeletal modeling. *J. Neural Eng.* 15, 066026. <https://doi.org/10.1088/1741-2552/aae26b>

- Sartori, M., Rubenson, J., Lloyd, D.G., Farina, D., Panizzolo, F.A., 2017. Subject-Specificity via 3D Ultrasound and Personalized Musculoskeletal Modeling, in: Ibáñez, J., González-Vargas, J., Azorín, J.M., Akay, M., Pons, J.L. (Eds.), *Converging Clinical and Engineering Research on Neurorehabilitation II*, Biosystems & Biorobotics. Springer International Publishing, Cham, pp. 639–642. [https://doi.org/10.1007/978-3-319-46669-9\\_105](https://doi.org/10.1007/978-3-319-46669-9_105)
- Saul, K.R., Hu, X., Goehler, C.M., Vidt, M.E., Daly, M., Velisar, A., Murray, W.M., 2015. Benchmarking of dynamic simulation predictions in two software platforms using an upper limb musculoskeletal model. *Comput. Methods Biomech. Biomed. Engin.* 18, 1445–1458. <https://doi.org/10.1080/10255842.2014.916698>
- Scheys, L., Spaepen, A., Suetens, P., Jonkers, I., 2008a. Calculated moment-arm and muscle-tendon lengths during gait differ substantially using MR based versus rescaled generic lower-limb musculoskeletal models. *Gait Posture* 28, 640–648. <https://doi.org/10.1016/j.gaitpost.2008.04.010>
- Scheys, L., Van Campenhout, A., Spaepen, A., Suetens, P., Jonkers, I., 2008b. Personalized MR-based musculoskeletal models compared to rescaled generic models in the presence of increased femoral anteversion: Effect on hip moment arm lengths. *Gait Posture* 28, 358–365. <https://doi.org/10.1016/j.gaitpost.2008.05.002>
- Schindelin, J., Arganda-Carreras, I., Frise, E., Kaynig, V., Longair, M., Pietzsch, T., Preibisch, S., Rueden, C., Saalfeld, S., Schmid, B., Tinevez, J.-Y., White, D.J., Hartenstein, V., Eliceiri, K., Tomancak, P., Cardona, A., 2012. Fiji: an open-source platform for biological-image analysis. *Nat. Methods* 9, 676–682. <https://doi.org/10.1038/nmeth.2019>
- Smith, S.H.L., Coppack, R.J., van den Bogert, A.J., Bennett, A.N., Bull, A.M.J., 2021. Review of musculoskeletal modelling in a clinical setting: Current use in rehabilitation design, surgical decision making and healthcare interventions. *Clin. Biomech.* 83, 105292. <https://doi.org/10.1016/j.clinbiomech.2021.105292>
- Stanev, D., Filip, K., Bitzas, D., Zouras, S., Giarmatzis, G., Tsaopoulos, D., Moustakas, K., 2021. Real-Time Musculoskeletal Kinematics and Dynamics Analysis Using Marker- and IMU-Based Solutions in Rehabilitation. *Sensors* 21, 1804. <https://doi.org/10.3390/s21051804>
- Tagliapietra, L., Vivian, M., Sartori, M., Farina, D., Reggiani, M., 2015. Estimating EMG signals to drive neuromusculoskeletal models in cyclic rehabilitation movements, in: 2015 37th Annual International Conference of the IEEE Engineering in Medicine and Biology Society (EMBC). Presented at the 2015 37th Annual International Conference of the IEEE Engineering in Medicine and Biology Society (EMBC), pp. 3611–3614. <https://doi.org/10.1109/EMBC.2015.7319174>

- Thelen, D.G., 2003. Adjustment of Muscle Mechanics Model Parameters to Simulate Dynamic Contractions in Older Adults. *J. Biomech. Eng.* 125, 70–77.  
<https://doi.org/10.1115/1.1531112>
- van Ravenzwaaij, D., Cassey, P., Brown, S.D., 2018. A simple introduction to Markov Chain Monte–Carlo sampling. *Psychon. Bull. Rev.* 25, 143–154.  
<https://doi.org/10.3758/s13423-016-1015-8>
- Winters, J.M., 1995. An improved muscle-reflex actuator for use in large-scale neuromusculoskeletal models. *Ann. Biomed. Eng.* 23, 359–374.  
<https://doi.org/10.1007/BF02584437>
- Xu, T., Liang, Y., Feng, L., Liu, L., Yeung, E., He, R., To, M., Hu, Y., 2025. Personalizing Muscle Tendon Parameters of Cerebral Palsy Patient’s Digital Model. *IEEE Trans. Neural Syst. Rehabil. Eng.* 33, 1079–1087.  
<https://doi.org/10.1109/TNSRE.2025.3544551>
- Zajac, F.E., 1989. Muscle and tendon: properties, models, scaling, and application to biomechanics and motor control. *Crit. Rev. Biomed. Eng.* 17, 359–411.
- Zhao, Y., Zhang, J., Li, Z., Qian, K., Xie, S.Q., Lu, Y., Zhang, Z.-Q., 2023. Computationally Efficient Personalized EMG-Driven Musculoskeletal Model of Wrist Joint. *IEEE Trans. Instrum. Meas.* 72, 1–10. <https://doi.org/10.1109/TIM.2022.3225023>
- Żuk, M., Syczewska, M., Pezowicz, C., 2018. Influence of Uncertainty in Selected Musculoskeletal Model Parameters on Muscle Forces Estimated in Inverse Dynamics-Based Static Optimization and Hybrid Approach. *J. Biomech. Eng.* 140.  
<https://doi.org/10.1115/1.4040943>

## APPENDICES

## Appendix A. Additional Statistics for Chapter 2

Table 2.3b: MSK Parameter Sensitivity Post-Hoc Analysis (Interactions)

<i>Parameter</i>	<i>Comparison Group 1</i>		<i>Comparison Group 2</i>		Mean Difference ± Standard Error	p-value
	Contraction Type	Effort Level	Contraction Type	Effort Level		
<i>Optimal Fiber Length</i>	Isometric	50%	Isometric	25%	0.020±0.009	0.064
	Isotonic	50%	Isotonic	25%	0.010±0.007	0.151
	Isotonic	25%	Isometric	25%	0.041±0.009	<b>0.002*</b>
	Isotonic	50%	Isometric	50%	0.011±0.015	0.495
<i>Tendon Slack Length</i>	Isometric	50%	Isometric	25%	0.021±0.028	0.462
	Isotonic	50%	Isotonic	25%	0.035±0.035	0.341
	Isotonic	25%	Isometric	25%	0.115±0.042	<b>0.023*</b>
	Isotonic	50%	Isometric	50%	0.101±0.025	<b>0.003*</b>
<i>Maximum Isometric Force</i>	Isometric	50%	Isometric	25%	0.015±0.016	0.371
	Isotonic	50%	Isotonic	25%	0.018±0.018	0.350
	Isotonic	25%	Isometric	25%	0.033±0.022	0.180
	Isotonic	50%	Isometric	50%	<0.001±0.020	0.966
<i>Pennation Angle</i>	Isometric	50%	Isometric	25%	0.004±0.003	0.230
	Isotonic	50%	Isotonic	25%	<0.001±0.007	0.925
	Isotonic	25%	Isometric	25%	0.052±0.008	<b>&lt;0.001**</b>
	Isotonic	50%	Isometric	50%	0.047±0.004	<b>&lt;0.001**</b>
<i>Muscle Fiber Damping</i>	Isometric	50%	Isometric	25%	<0.001±0.004	0.953
	Isotonic	50%	Isotonic	25%	0.010±0.003	<b>0.008*</b>
	Isotonic	25%	Isometric	25%	0.018±0.005	<b>0.005*</b>
	Isotonic	50%	Isometric	50%	0.008±0.005	0.177

## Appendix B. Comparison of Movement Type NRMSE from Chapter 3

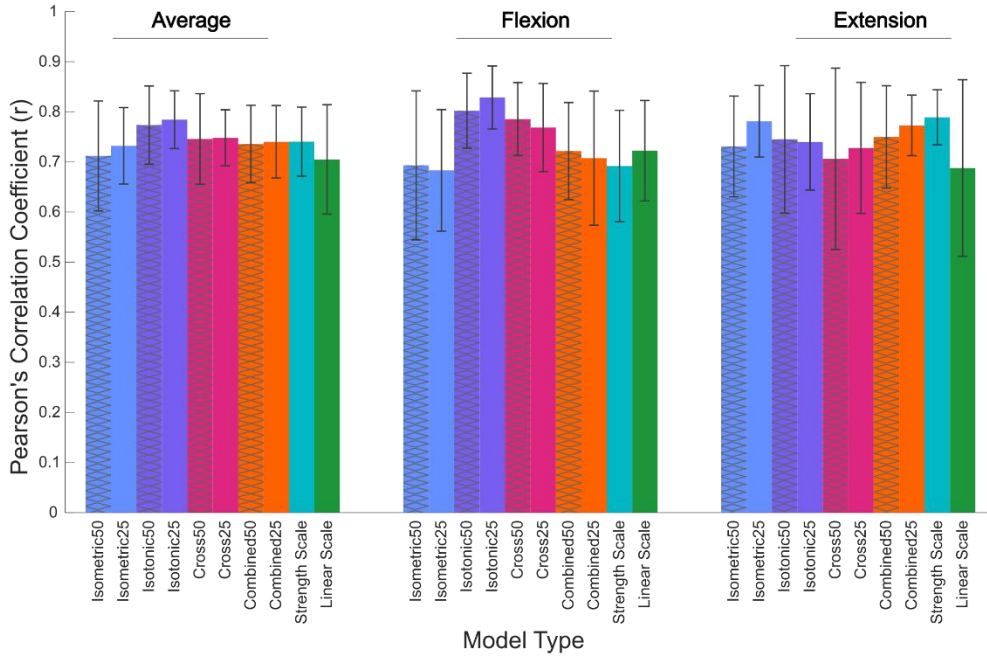


**Figure 3.3b** Average Pearson's correlation coefficients of each optimized model and control model type for flexion and extension movements. The coefficients and their standard deviations presented here are the composite coefficients for all evaluation data sets.

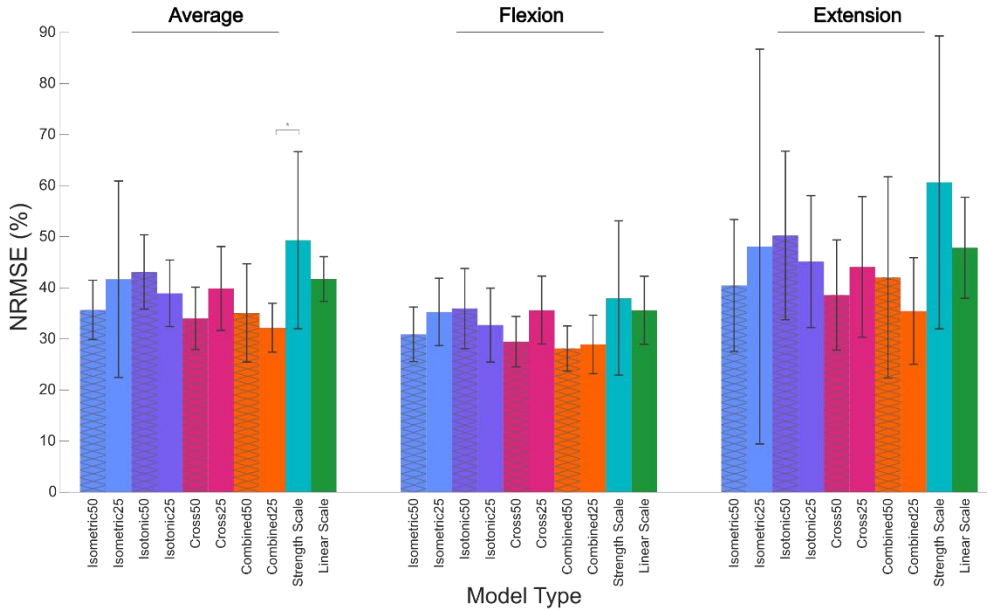


**Figure 3.4b** Normalized root mean squared error of each optimized model and control model type for flexion and extension movements. The NRMSE and standard deviations presented here are the composite NRMSE for all evaluation data sets.